Investigating the Circadian Regulation of the Inner Blood Retinal Barrier in Early and Intermediate Age-Related Macular Degeneration

A thesis submitted to The University of Dublin for the degree of Master of Science 2021

By Dr Aisling Naylor

MB, BCh, BAO

Supervisor: Dr Matthew Campbell

Department of Genetics

Trinity College Dublin

Declaration:

I declare that this thesis has not been submitted as an exercise for a degree at this or any other university and it is entirely my own work.

I agree to deposit this thesis in the University's open access institutional repository or allow the library to do so on my behalf, subject to Irish Copyright Legislation and Trinity College Library conditions of use and acknowledgement.

Aisling Naylor

March 2021

Trinity College Dublin
Coláiste na Tríonóide, Baile Átha Cliath
The University of Dublin

Summary:

Age-related macular degeneration (AMD) is the leading cause of central visual impairment worldwide with an estimated 196 million people with the condition in 2020 and a projected increase in prevalence as a result of exponential aging. AMD leads to the painless, progressive loss of central vision which we require for essential tasks such as reading and recognising faces. AMD is a multifactorial condition characterised by macular photoreceptor loss and retinal pigment epithelium (RPE) cell reduction. AMD is classified into two distinct forms known as "dry" AMD or "wet" AMD. Geographic atrophy (GA) is the advanced form of dry AMD; features of GA include damage to outer retinal structures including localised RPE atrophy, photoreceptor cell death and choriocapillaris atrophy. Wet AMD, which is also known as neovascular AMD or exudative AMD is characterised by choroidal neovascularisation (CNV); the growth of new blood vessels from the underlying choroid into the RPE or subretinal space leading to haemorrhage or oedema and a sudden decrease in visual acuity. There are currently no treatments available for GA apart from lifestyle changes such as dietary modification and smoking cessation. The progression of early AMD into GA or CNV is unpredictable and despite wealth of research into AMD the molecular pathology underlying the condition remains unclear thereby limiting potential therapies.

The retina and the RPE are especially prone to the development of reactive oxygen species leading to the accumulation of toxic substances in photoreceptor cells. As a result, photoreceptor cells undergo a constant renewal process with their outer segments being shed daily. This process is tightly coordinated in order to maintain a constant length of photoreceptor outer segments. Some of the phagocytosed material is recycled back to the photoreceptors and the remainder is exocytosed by the RPE and likely cleared by choriocapillaris. The major burst of phagocytic activity is under the control of the circadian clock. Dysfunctional rates of clearance of these components are likely a significant factor to drusen accumulation and subsequently the development of AMD in some individuals.

Drusen are the characteristic pathological feature associated with AMD. They are extracellular deposits of lipids, proteins, iron and zinc located between the RPE and Bruch's membrane. There is a wide variety in the size and distribution of drusen from individual to individual however there is symmetry in drusen size, number, density and fluorescence between eyes within an individual. This correlates with a high degree of symmetry of retinal blood vessel patterning in the eyes of an individual. Tight junctions (TJs) in the retinal vasculature form the inner blood retinal barrier (iBRB) which is essential for the maintenance of retinal homeostasis and preventing the entry of potentially damaging blood borne agents. Hudson *et al* 2019 have demonstrated that the gene CDLN-5 is regulated by BMAL1 and the

circadian clock. CDLN-5 encodes for claudin-5, one of the most enriched tight junction proteins in the iBRB. They demonstrated that persistent suppression of claudin-5 in mice exposed to a cholesterol enriched diet produced striking RPE atrophy. Similarly, suppression of claudin-5 in the macular region of non-human primates induced RPE cell atrophy. Furthermore, fundus fluorescein angiography (FFA) in healthy human subjects demonstrated an increased permeability of the iBRB in the evening compared to the morning. These findings indicate that there may be an inner-retina derived component in the early pathophysiological changes associated with AMD and suggests that regulating the dynamic expression pattern of claudin-5 at the iBRB could control the burden of material consumed by the RPE daily. AMD is considered a disease of the outer retina and for this reason the majority of research to date has focused on identifying pathological determinants in RPE cells. To our knowledge this is the first time an inner-retinal derived contribution to RPE cell atrophy has been demonstrated. Overall these findings directly implicate claudin-5 as a key mediator of subsequent RPE pathology and suggest that methods aimed at restoring the dynamic expression of this molecule in the aging eye may prevent or attenuate the progression of AMD.

To continue the clinical portion of this research, we are making a full assessment of circadian iBRB regulation in patients with defined degrees of dry AMD and age-matched controls. We have performed quantitative FFA and optical coherence tomography (OCT) in the morning and the evening in the same individual to assess retinal blood vessel integrity and retinal thickness changes. We have also screened participants' blood samples at both timepoints to correlate any potential changes in inflammatory status, melatonin and cortisol levels and circadian mediated changes in clock components with barrier integrity at particular times of day. In addition, participants will have DNA isolated and subsequently genotyped for AMD risk variants such as Complement Factor H (CFH), Complement Factor B (CFB), Age-Related Maculopathy Susceptibility 2(ARMS2)/ High-Temperature Requirement A Serine Peptidase 1 (HTRA1) and Apolipoprotein E (APOE) to determine if there is a link between severity of disease, risk variant and changes in iBRB integrity or vessel permeability. In gaining an understanding of circadian regulation of the iBRB in a clinical setting in human subjects, we will be positioned to make profound conclusions on its role in AMD pathophysiology, aiding our understanding of GA pathophysiology and potentially, in the future, development of therapeutic strategies to treat the condition.

Acknowledgements:

I would like to thank Dr Matthew Campbell for his support, enthusiasm and encouragement throughout the course of my research. I also wish to express my gratitude to Mr Mark Cahill for facilitating this project and for his mentorship both in the academic and clinical aspects of this research. Many thanks to Dr Natalie Hudson for her advice, diligence and for dedicating so much of her time to this project, especially for the early mornings and late evening testing sessions. To Dr Jeffery O'Callaghan, sincerest thanks for all your work in designing and implementing of our automated FFA programme. I would also like to pay special regards to the other members of the Campbell Laboratory including Dr. Yosuke Hashimoto, Conor Delaney, Dr. Chris Greene, Nicole Hanley, and Claire O'Connor as well as Dr Sophie Kiang. Furthermore, many thanks to Dr Alan Hopkins for his encouragement and advice and for all his work in commencing this research.

Thanks to Dr Paul Kenna, Roisin Clarke and the Research Foundation in The Royal Victoria Eye and Ear Hospital along with the Irish College of Ophthalmologists and Novartis for supporting my project.

Finally, thank you to Siobhain and to my family.

Table of Contents:

CHAPTER 1: Introduction

1.1. The Retina and Photoreceptor cells

The retina is located at the posterior pole of the eye between the vitreous and Bruch's membrane and consists of two primary layers: an inner neurosensory retina and an outer retinal pigment epithelium (RPE). The neurosensory retina converts light stimuli into neural impulses, these are partially integrated locally and transmitted to the brain via ganglion cell axons in the optic nerve. Retinal cells include neural cells (photoreceptors, bipolar cells and ganglion cells), glial cells, vascular endothelium, pericytes and microglia (Forrester *et al.,* 2015). These cells are arranged in a highly organised matter and in histological sections appear as distinct layers as illustrated in Figure 1a (Naylor *et al.* 2019). There are three types of photoreceptor cells in the eye: rods, cones and intrinsically photosensitive retinal ganglion cells. Rods and cone cells are found in the outermost layer of the retina. There are approximately 115 million rods and 6.5 million cones in the human eye (Forrester *et al*., 2015). Rods are responsible for sensing contrast, brightness and motion and cones for sensing fine resolution, spatial resolution and colour vision (Forrester *et al*., 2015). The density of rods and cones varies in different regions of the retina; the peripheral retina is rod dominated, with a maximum rod density in the perifovea and an absence in the fovea. Cone density increases at the macula and the fovea is composed of solely of cones (Sundaram *et al.* 2016). The outer segments of rods and cones contain flattened discs containing light sensitive visual pigments responsible for the absorption of light and initiation of the neuroelectrical impulse, these must be regenerated after photon capture (Forrester *et al.,* 2015, Fritsche *et al.,* 2014).

The retinal pigment epithelium (RPE) is a single layer of epithelial cells located between the Bruch's membrane and the photoreceptor layer of the retina. The RPE provides a unique support system to the photoreceptors by delivering resources needed to carry out visual function and recycling retinoids for phototransduction. The RPE has many other functions which include: maintaining adhesion of the neurosensory retina; providing a selectively permeable barrier between the choroid and neurosensory retina; phagocytosis of rod outer and to a lesser extent cone outer segments; synthesis of interphotoreceptor matrix; absorption of light scatter and transport plus storage of metabolites and vitamins (Sparrow *et al*., 2010, Strauss, 2005, Forrester *et al.,* 2015) as illustrated in Figure 1b (Naylor *et al.,* 2019). The RPE is highly polarised with its basal surface resting on Bruch's membrane and its apical villi enveloping the photoreceptor outer segments (Shin *et al.* 2006). The basolateral surface acts as a barrier between the neuroretina and the highly permeable choriocapillaris forming the outer blood retinal barrier (oBRB) (Sparrow *et al.,* 2010, Simo *et al*., 2010, Maneros *et al.,* 2005).

Bruch's membrane is a modified connective tissue layer located between the RPE and choroid (Forrester *et al.,* 2015).

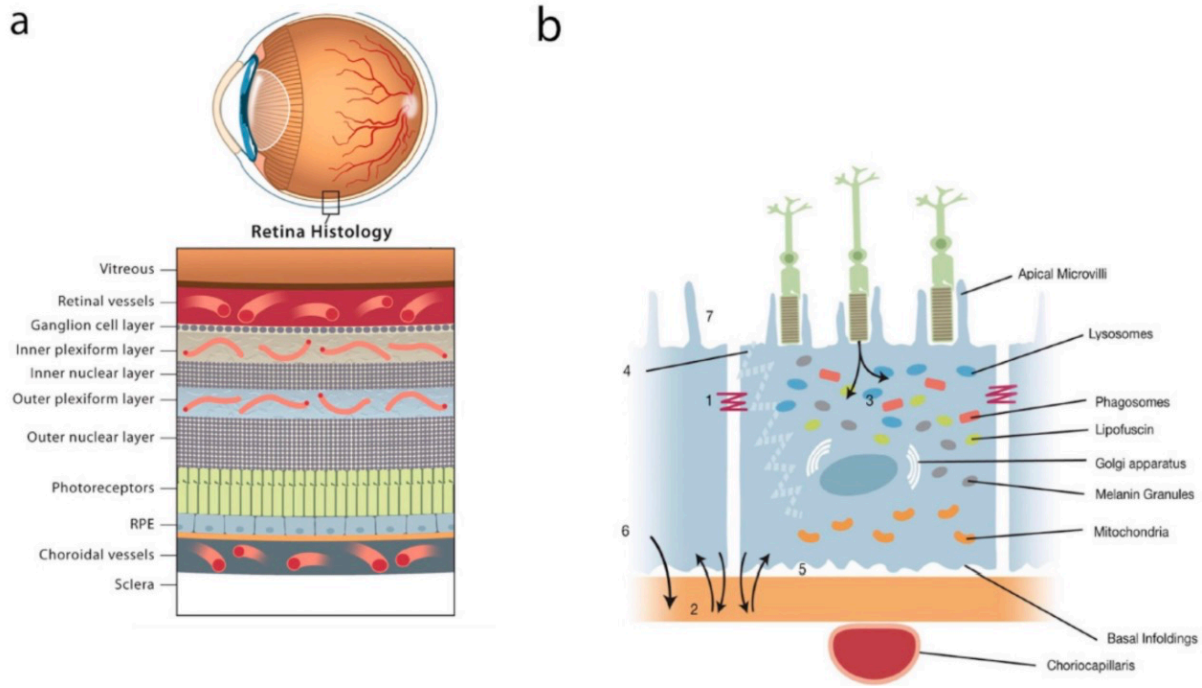

Figure 1.1 a. Topographic relationship of the retinal pigment epithelium (RPE) within the retina.
Figure 1.1 b. RPE anatomy and function. The functions of the RPE are labelled as follows: (1) Tight junction (TJ) of the outer blood retina barrier (oBRB); (2) Transport of fluid, nutrients, and metabolites (paracellular and transcellular); (3) Phagocytosis of photoreceptor outer segments (POS); (4) Absorption of scattered light; (5) Retinal adhesion; (6) Paracrine secretion (including vascular endothelial growth factor (VEGF)); (7) Maintaining balance across the sub-retinal space.
(Taken from Naylor *et al.,* 2019).

1.2. The Macula

The macula lies in the posterior pole of the eye and is defined as the area of the retina bound by the superior and inferior vascular arcades. The macula is roughly 4.5mm in diameter and is located 3mm temporally to the optic disc. The macula can be subdivided into the foveola, the fovea, the parafovea and the perifovea (Sternberg Jr *et al.,* 2017). The fovea is the central area of the macula and measures 1.5mm in diameter (Sternberg Jr *et al.,* 2017, Forrester *et al*., 2016). The macula has a yellow appearance due to the presence of xanthophyll carotenoid pigments. (Sternberg Jr *et al*., 2017). As the name suggests AMD preferentially targets the macular region of the retina, however the mechanistic rational for this is not known.

1.3. Retinal blood supply

The retina is extremely metabolically active with the highest oxygen concentration per weight of any organ. The retina has a dual blood supply with its inner two-thirds supplied by branches of the central retina vessels and its outer one-third supplied by the choroidal circulation (Forrester *et al*., 2015). The larger branches of the central retinal artery and vein lie below the internal limiting membrane and are surrounded by astrocytes, pericytes and retinal muller cells (Daruich *et al.,* 2018). The capillaries pass only as far as the inner nuclear layer, therefore the outer retina is normally avascular. The choroid is an extensive vascular complex located between the sclera and retina and divided into Sattler's layer composed of medium and small sized vessels and Haller's layer composed of large arteries (Daruich *et al.,* 2018, Forrester *et al.,* 2015). The inner portion of the choroid is a network of fenestrated capillaries that supply nutrients to the retina and act as a conduit for the by-products of PR and RPE metabolism (Fritsche *et al.,* 2014).

1.4. The Blood Retina Barrier

The retina has a highly selective blood-tissue barrier, the blood retina barrier (BRB) which is fundamental in establishing and maintaining an environment for optimum retinal function (Cunha-Vas *et al.,* 2011). The BRB is comprised of the inner BRB (iBRB) which is formed by tight junctions (TJs) between retinal capillary endothelial cells and the outer blood retina barrier (oBRB) which is formed by TJs between RPE cells (Cunha-Vas *et al.,* 2011). The BRB is a restrictive physical barrier which regulates ion, protein and water flux into and out of the retina. TJs between adjacent cells restrict the paracellular movement of plasma components and toxic molecules in to and out of the retina. Both the oBRB and iBRB perform similar roles of paracellular diffusion regulation however their molecular composition varies (Cunha-Vas *et al.,* 2011).

TJs are unique assemblies of transmembrane proteins and peripheral cytoplasmic proteins that interact with each other to form a complex network and allow for a high degree of paracellular selectivity. Transmembrane proteins include the claudins, the MARVEL (Mal and related proteins for vesicle trafficking and membrane link) family and junctional adhesion molecules (JAMs), which span the plasma membrane (Gonzalez-Mariscal *et al.,* 2000). These extend into the paracellular space creating a seal characteristic of TJs (Campbell and Humphries, 2013). Peripheral cytoplasmic proteins such as zonula occludens-1, (ZO-1), -2 (ZO-2) and -3 (ZO-3) anchor these transmembrane proteins to the plasma membrane and are vital in the initial formation and distinct organization of TJs (Bazzoni *et al*., 2000, Bazzoni *et al*., 2004).

Claudins are the main proteins involved in TJ strand formation and they directly regulate permeability, selectivity and mediate robust cell-cell adhesion (Shin *et al.,* 2006, Colegio *et al.,* 2003, Rizollo *et al.,* 2011). There are 24 established members of the claudin family (Shin *et al.,* 2006) and each member has a unique effect on permeability and selectivity. In fact, specific paracellular properties of different epithelia results from their particular patterns of claudin expression (Colegio *et al.,* 2003, Saitou *et al*., 2000). In humans, claudin-1, -2 and -5 are the most important in the endothelial cells of iBRB (Daruich *et al.,* 2018) and claudin-3, claudin-10 and claudin-19 have been detected in the RPE (Peng *et al.,* 2010). Some claudins are expressed in a tissue specific manner, for example claudin-5 is expressed predominantly endothelial cells (Morita *et al.,* 1999) and is necessary to preserve the vascular barrier to small (<0.8 kDa) molecules in the brain (Nitta *et al*., 2003). Claudin-5 is the most enriched component of both the brain and retinal endothelial tight junction (Daneman *et al.,* 2010) and is of particular importance to our study as we will discuss further in this chapter.

1.5. Prevalence and Natural History of AMD

AMD is the leading cause of visual impairment in the developed world and accounts for 90% of severe vision loss in Ireland (HSE Model of Eye Care, 2017). Current CSO projections for Ireland estimate that the number of people aged 65 years or older will almost double over the period of 2006 to 2026, therefore the number of people in Ireland with sight loss will increase exponentially as the population ages (HSE Model of Eye Care, 2017). In 2017 there were 225,000 people living with sight loss in Ireland and this was thought to increase to 272,000 by 2020 (HSE model of Eye Care, 2017). Globally, the prevalence of AMD is likely to increase from a projected 196 million people with AMD in 2020 to 288 million in 2040 (Wong *et al.,* 2014). Klein *et al.,* 2002 demonstrated that 9.5% of people aged over 75 years old developed late signs of Age-Related Maculopathy (ARM). Not only does visual impairment significantly reduce quality of life by affecting physical, emotional, functional and social wellbeing but also contributes to significant financial costs with the financial and economic costs of blindness in the Republic of Ireland expected to increase from €276.6 million and €809 million respectively in 2010 to €367 million and €1.1 billion respectively in 2020 (Green *et al*., 2016).

AMD leads to the progressive, painless loss of central visual function. As clinical signs such as drusen and pigmentary changes may precede visual loss, early AMD is often diagnosed incidentally during the course of a routine eye examination. Visual impairment secondary to AMD has major impact on the quality of life in individuals with the condition; from the inability to undertake tasks that require visual discrimination such as reading, driving and

recognising faces to the ability to perform activities of daily living (Gopinath *et al.,* 2014). Individuals with AMD report greater life stress lower activity levels and increased depression compared to those without AMD (Casten *et al.,* 2018).

AMD is characterised by the degeneration of various structures at the posterior pole of the eye including the outer retina, the RPE, Bruch's membrane and the choriocapillaris. AMD is classified into two distinct forms known as "dry" AMD or "wet" AMD. Geographic atrophy (GA) is the advanced form of dry AMD; features of AMD include damage to outer retinal structures including sharply delineated, localised RPE atrophy, photoreceptor cell death and choriocapillaris atrophy (Sternberg Jr *et al.,* 2017, Fleckenstein *et al.,* 2018, Arya *et al.,* 2018). GA leads to progressive, irreversible vision loss accounting for 10% of severe visual loss from AMD (Sternberg Jr *et al.,* 2017). GA is generally bilateral, and lesions affect the perifoveal macula first, sparing the foveal centre until lesions gradually enlarge and coalesce to include the fovea. The degree of visual loss depends on the location of GA with respect to the fovea or central macula and patients may often demonstrate good visual acuity as a result of foveal sparing (Sternberg Jr *et al.,* 2017). Wet AMD, which is also known as neovascular AMD or exudative AMD is characterised by choroidal neovascularisation (CNV), the growth of new blood vessels from the underlying choroid into the RPE or subretinal space leading to haemorrhage, exudative retinal detachment and serous or haemorrhagic pigment epithelial detachments (Sternberg Jr *et al.,* 2017, Cook *et al.,* 2008). Patients with wet AMD generally present with a sudden decrease in central vision, often with distortion (Cook *et al.,* 2008). Wet AMD accounts for 75% of severe visual impairment secondary to AMD despite representing only 10-15% of total AMD cases (Sundaram *et al.,* 2016, Cook *et al.,* 2008).

1.6. Clinical Examination, Grading and Treatment of AMD

Clinical assessment of AMD involves best corrected visual acuity (BCVA), slit lamp fundal examination and retinal imaging including fundal photography, optical coherence tomography (OCT), fundus autofluorescence (FAF) and fundus fluorescein angiography (FFA). BCVA may often underestimate functional deficits in AMD, particularly relevant for GA where a patient's BCVA may be preserved due to foveal sparing (Fleckenstein *et al.,* 2018). OCT is used to assess macular thickness, RPE integrity, the presence of fluid collections and to determine the response to treatment. FAF provides invaluable information about the health of the RPE and in early AMD, can reveal areas of RPE alterations which are not visible on fundoscopy (Ly *et al.,* 2017). FFA imaging examines both retinal and choroidal circulation and allows for the visualisation of blood vessels and CNV (Cook *et al.,* 2008). The fenestrated

walls of the choriocapillaris allow free fluorescein to pass through whereas the iBRB does not allow any physiological fluorescein leakage (Sundaram *et al.,* 2016).

Many classification systems exist in order to determine the severity of AMD, these include the AREDS scale and the International Classification and Grading system for age related maculopathy which are both based on colour fundus photography. It is important to accurately classify AMD as this will determine the risk of progression of AMD and treatment options. The AREDS scale is based on drusen characteristics (size, type, area), pigmentary abnormalities (increased pigment, depigmentation, geographic atrophy (GA)) and presence of abnormalities characteristic of neovascular AMD. Advanced AMD was defined as the presence of one of more neovascular AMD abnormalities, photocoagulation for AMD or GA involving the centre of the macula. It comprises a 9-step severity scale combining a 6-step drusen area scale and 5-syep pigmentary abnormality scale. For ease of classification, the AREDS simplified severity scale was produced (Ferris *et al.,* 2005) which allocated one risk factor for the presence of one or more large drusen (≥125μm or the width or a large vein at disc margins) and one risk factor for the presence of any pigmentary abnormality. These risk factors were summed across both eyes yielding a 5-step scale (0-4) on which the approximated 5-year risk of developing advanced AMD In at least one eye increases in this sequence:

0 factors 0.5%

1 factor 3%

2 factors 12%

3 factors 25%

4 factors 50%

The distinction between wet and dry AMD is important in relation to the treatment pathways for the condition. Over the last two decades there have been major advances in the treatment of CNV with the advent of intravitreal injections targeting vascular endothelial growth factor (VEGF). Pegaptanib (Macugen) was the first anti-VEGF licensed by the Food and Drug Administration (FDA) in the US in the treatment of AMD (Sternberg Jr *et al.,* 2017). In 2006, a landmark trial demonstrated that monthly injections Ranibizumab (Lucentis) prevented vision loss in nearly 95% of patients and significantly reduced vision loss in 40% (Rosenfeld *et al.,* 2006). Other anti-VEGF agents include Bevacizumab (Avastin) and Aflibercept (Eylea). Despite these advances in the treatment of neovascular AMD there are currently no available treatments for GA. Patients with visual loss secondary to GA are encouraged to use low vision aids and make lifestyle modifications including cessation of smoking, dietary changes with an increased intake of leafy green vegetables and advised to

take supplements such as macushield and lutein omega. The Age-Related Eye Disease Study (AREDS) (AREDS Report no. 8, 2008) was developed to assess the benefits of antioxidants (500mg Vitamin C, 400IU vitamin E, 15mg beta-carotene) and 80mg zinc (2mg copper) in the prevention of AMD progression. This study found that patients treated with antioxidants and zinc in categories 3 (a minimum of extensive intermediate drusen or at least 1 large druse present) and 4 (advanced AMD or vision loss from AMD in one eye) experienced a significant reduction in the risk of AMD progression (25%) compared to those receiving a placebo.

1.7. Pathogenesis of AMD

1.7.1. Normal retinal homeostasis

The retina and the RPE are particularly prone to the generation of reactive oxidative species (ROS) as they have a high metabolic rate, a high concentration of polyunsaturated fatty acids and are exposed to constant light energy and high oxygen levels (Chakravarthy *et al.,* 2010, Fanjul-Moles *et al.,* 2015). As a result, toxic substances accumulate in photoreceptor cells daily. The rod outer segments undergo a constant renewal process whereby they are regenerated over 7-12 days (Strauss *et al.,* 2005, Sparrow *et al.,* 2012). In fact, 10% of photoreceptor outer segments (POS) are phagocytosed daily and new POS are built (Crabb *et al.,* 2002). Shed POS are phagocytosed by the RPE thereby allowing for essential molecules to be recycled back to the photoreceptors (Simo 2010, Strauss *et al* 2005). This process of disc shedding, phagocytosis and the formation of new photoreceptor outer segments is tightly coordinated in order to maintain a constant length of the POS (Strauss, 2005). Not all the components of the shed POS are recycled however, and some are cleared via the choriocapillaris (Boyle *et al.,* 1991). Oxidative stress plays a vital role in AMD with age-related cumulative damage in the RPE occurring due to an imbalance between the production and elimination of reactive oxygen species (ROS). Lipofuscin are retinal waste products from remnants of photoreceptor outer segment membranes, they accumulate in the RPE and are suspected to be the primary source of ROS in AMD and play a role in its exacerbation (Fanjul-Moles *et al.,* 2015, Sparrow *et al.,* 2010). Dysfunctional rates of clearance of these components are likely a significant factor to drusen accumulation in some individuals (Kim *et al*., 2013, Yao *et al.,* 2018). Significantly, this process of rod outer segment shedding is under control of the circadian clock with the major burst of phagocytosis taking place soon after the onset of light (LeVail*.,* 1976). This is reflected by a significant increase in the number of phagosomes at this time (LeVail*,* 1976).

1.7.2. Risk factors for the development of AMD

AMD is a complex, multifactorial condition with a varied rate of progression between individuals. Multiple risk factors have been identified for the development and progression of AMD including advancing age, genetic risk variants, lifestyle and environmental factors and phenotypic risk factors (Chakravarthy *et al.,* 2010). As the name implies, age is the most important risk factor for the development of AMD (Chakravarthy *et al.,* 2010). Aging is associated with structural and functional changes to the retina predisposing to the development of AMD (Ehrlich *et al.,* 2008). Significantly, aging is associated with a 30% loss of all rod photoreceptors and Bruch's membrane thickening due to the accumulation of apolipoproteins B and E and cholesterol (Curcio *et al.,* 2000). This thickening acts as a potential stimulus for inflammation and in combination with age related reduction in choroidal thickness leads to impaired transport of fluids and nutrients to photoreceptors (Curcio *et al.,* 2000, Fritsche *et al.,* 2014, Garcia-Layana *et al.,* 2017). Furthermore, there is an age-related decline in POS phagocytosis by the RPE leading to lipofuscin accumulation, ROS production and the subsequent loss of RPE cells (Garcia-Layana *et al.,* 2017). Aging, in the presence of other risk factors including ethnicity, smoking, diet, and genetic variants increases likelihood of AMD development.

Multi-ethnic studies show differing prevalence rates of any form of AMD between ethnic groups with a prevalence of 2.4% in an African population, 4.2% in an Hispanic population, 4.6% in a Chinese population and 5.4% in Caucasians (Heesterbeek *et al*., 2020). In agreement with this Cook *et al.,* 2008 report that there is a higher prevalence of AMD in the European population and Wong *et al.,* 2014 demonstrate that there is a higher prevalence of early AMD in Europeans than in Asians, however a similar prevalence of late AMD in the two demographics. Smoking is a modifiable risk factor associated with AMD. There is a strong association between smoking, development of AMD and progression to late AMD (Cook *et al.,* 2008, Velilla *et al.,* 2013, Mitchell *et al.,* 2002, Connelly *et al.,* 2018). Cigarette smoke contains toxic compounds that promote oxidative damage, impair the choroidal circulation and activate the immune system thereby predisposing individuals to the development of AMD (Garcia-Layana *et al.,* 2017, Velilla *et al.,* 2013, Heesterbeek *et al.,* 2020). It should be noted that many of the environmental and genetic risk factors associated with AMD are also associated with other multifactorial degenerative diseases of advanced age, including cardiovascular disease, Alzheimer's disease and Parkinson's disease (Pennington *et al.,* 2016, Heesterbeek *et al.,* 2020). However, the association between AMD and lipid/ cardiovascular factors including cardiovascular disease, stroke, atherosclerosis, hypertension and lipid levels have been inconclusive (Heesterbeek *et al.,* 2020, Pennington *et al.,* 2016). Having a higher

body mass index (BMI) was found to increase the probability of developing AMD in some studies while others found no association (Heesterbeek *et al.,* 2020). Diet has been found to play a possible role in the prevention of/ or delay of progression of AMD with dietary intake of long-chain polyunsaturated fatty acids (FA), fish and food rich in antioxidants lowering AMD risk (Sternberg Jr *et al.,* 2017, Heesterbeek *et al.,* 2020). Physical activity may confer a retinal health benefit as regular exercise is thought to increase antioxidant activity. Indeed, some studies demonstrate an association between physical activity and low odds of both early and late AMD (Heesterbeek *et al.,* 2020).

Genes play an important role in the development of AMD and the genetic susceptibility to AMD development and progression is further modified by environmental factors. Studies of the genetic associations of AMD have contributed significantly to the current knowledge of AMD pathology. Half of the genomic heritability can be accounted for by common and rare genetic variants in 34 genetic loci (Heesterbeek *et al.,* 2020, Mitchell *et al.,* 2018). These can be grouped into different biological pathways including those involved in the complement system (Complement factor H *(CFH)*, Complement component 2 (*C2)*, Complement factor B (*CFB)*, Complement factor inhibitor (*CFI)*, Complement component 3 (*C3)*, and complement component 9 (*C9*); lipid metabolism (apolipoprotein E (*APOE*)); extracellular membrane remodelling (tissue inhibitor of matrix metalloproteinase activity 3 (TIMP3), high-temperature requirement A serine peptidase (HTRA1)) and cell survival including DNA repair, apoptosis and the stress response (Age-related maculopathy susceptibility 2 (*ARMS2))* (Fritsche *et al.,* 2014). The major AMD associated genetic variants are CFH rs1061170, ARMS2 rs1040924, C3 rs2230199, CFB rs64 1153 and Superkiller viralicidic activity 2-like (SKIV2L) rs429608 (Connelly *et al.,* 2018). In an Irish population, the presence of CFH and ARMS2 and older age are two main risk factors associated with the prevalence of AMD (Connelly *et al.,* 2018). Homozygosity for minor the allele of either CFH or ARMS2 was a strong indicator of early AMD while heterozygosity for ARMS2 proved a strong indicator for late AMD. Carrying the CFH allele either as a homozygote or heterozygote strongly predicted progression within the early stages of AMD and progression to late AMD (Connelly *et al.,* 2018). CFH is a major inhibitor of the complement pathway (Fanjul-Moles *et al.,* 2015) and *CFH Y402H* polymorphism is strongly associated with AMD, playing a role in almost 60% of AMD at the population level (Garcia-Layana *et al.,* 2017).

Where other risk factors such as age, demographics and environmental risk factors are more valuable at earlier disease stages, phenotypic risk factors are of particular importance in predicting disease progression (Heesterbeek *et al.,* 2020). The Beaver Dam eye study (Klein *et al.,* 2002) investigated the 10-year incidence and progression of ARM demonstrating that eyes with soft indistinct drusen or RPE changes at baseline were more likely to develop late AMD at

follow up than eyes without these lesions. This study also demonstrated that soft drusen and pigmentary abnormalities significantly increase the risk for the development of geographic atrophy (GA) and exudative macular degeneration. The AREDS study was in agreement with this stating that large drusen and pigment changes were particularly predictive of developing advanced AMD (AREDS Report no. 8). Connelly *et al.,* 2018 demonstrated that 75% of those who progressed from early to late disease over a four-year period had soft drusen and hyperpigmentation at baseline.

It is likely that combinations of aging, the environment and protective or risk variants all influence the photoreceptor support system and determine the age of onset and severity of AMD (Fritsche *et al.,* 2014) however the exact role of these factors remains unknown.

1.7.3 Histopathology and Macular Translocation Surgery

The unpredictable nature of the progression from early AMD to GA or CNV or both and the devastating effects on patients' visual acuity and quality of life reinforce the need for a greater understanding of the pathogenesis of the condition. Understanding of the biology and pathophysiology at present, remains limited, which in turn limits therapies (Fritsche *et al.,* 2005). To date there have been two main histopathologic theories regarding the onset of AMD. One theory implicates the RPE as the primary site of damage with resultant choriocapillaris degeneration and photoreceptor loss whereas the other theory suggests that choroidal vascular insufficiency causes reduced clearance of waste from the extravascular space leading to secondary RPE and photoreceptor degeneration (McLeod *et al.,* 2009, Bird *et al.,* 1992, Curcio *et al.,* 1996). It is important to note that both of these theories are based on the end results of advanced AMD, attempting to work back from this end point. However, the results of macular translocation surgery challenges these hypotheses as it suggests a different primary site of damage other than that directly involving the outer retina and choriocapillaris.

Macular translocation surgery has been performed for both CNV and GA with the intention of restoring visual acuity by detaching the healthy neurosensory retina from the subretinal lesion, rotating it away from the damaged RPE and choriocapillaris and allowing the retina to be supported by healthy RPE and choroid. This has demonstrated positive results in in patients with subfoveal CNV. However, in eyes with GA that underwent macular translation surgery, the RPE atrophy reoccurred, initially as mild RPE changes and progressing to frank RPE atrophy a year post-operatively (Cahill *et al.,* 2005). The recurrence was continuous with the original pre-operative atrophic area and the dimensions were similar to those of the original areas of GA. The recurrence of GA suggests that primary pathology in AMD therefore may not

in fact lie in the choriocapillaris or the RPE but in the tissues implanted in this procedure. If GA is a panretinal condition, repositioning of more densely packed and metabolically demanding cells over peripheral cells may be sufficient to lead to RPE cell loss. Cahill *et al.,* 2005 also suggest that the primary defect in GA may arise from the photoreceptors leading to RPE death. If this is the case, then translocation of the defective sensory macula could result in accelerated damage to defective RPE that it is replaced over. It should be noted that in many diseases, abnormalities manifest downstream of the primary effector. We suggest that there is an inner blood retinal barrier derived mechanism of damage to the outer retina leading to AMD.

1.8. Drusen

Drusen are focal deposits of extracellular debris located between the basal lamina of the RPE and the inner collagenous layer of Bruch's membrane (Rudolf *et al.,* 2008). Drusen are composed of lipids which comprise >40% of drusen volume (including neutral lipids with esterified and unesterified cholesterol), proteins including complement proteins (C3, C3d, C3dg, C3b, C5, C6, C7, C8, C9, C5b-9 (MAC)), complement activators (β-amyloid and CRP), complement regulatory proteins (vitronectin and clusterin), TIMP3 and apolipoproteins (E, B, A-I, C-I, and C-II) plus zinc and iron ions (Fritsche *et al.,* 2014, Mitchell *et al.,* 2018, Wang *et al.,* 2010). Drusen lipids appear to be derived primarily from the RPE and photoreceptors, with a small contribution from the choroid blood supply whereas drusen proteins appear to come from both choroidal cells and serum with contributions from the RPE (Chakravarthy *et al.,* 2010, Crabb *et al.,* 2002, Curcio *et al.,* 2009). Diet derived lipoproteins (linolate) rather than photoreceptor derived lipoproteins (docosahexaenoate) are thought to dominate lipoprotein fatty acids in drusen (Curcio, 2018).

AMD is a bilateral condition, and although there is a wide variety in drusen patterning between individuals, there is remarkable symmetry in drusen size, number, density and fluorescence between eyes within an individual (Mann *et al.,* 2011, Bird, 1992, Barondes *et al.,* 1990). Barondes *et al.,* 1990 have suggested that the symmetry of drusen may result from metabolic malfunction specific to the individual rather than the non-specific result of aging.

Pseudodrusen which are also known as subretinal drusenoid deposits are located between photoreceptors and the RPE. Reticular pseudodrusen (RPD) consist of membranous debris, unesterified cholesterol, apolipoprotein E, complement factor H and vitronectin. RPD consist of differing lipid constituents than conventional drusen suggesting a different origin of the lipids in the two forms of deposit (Wightman and Guymer, 2019). RDP are an exact mirror of the topography of rod photoreceptors in the human macula (Curcio *et al.,* 2018) and

functional testing has demonstrated scotopic deficits, implicating rod photoreceptor deficiencies in RPD (Wightman & Guymer 2019). RPD can appear in eyes with no RPE pathology but are more common in AMD and are highly correlated with end stage disease phenotypes (Wightman and Guymer, 2019). Pseudodrusen have been found to confer a risk of AMD progression independent of drusen (Fritsche *et al.,* 2014) and for this reason it has been suggested that pseudodrusen should be considered along with the AREDS severity score for predicting late AMD. There are similar risk factors for both drusen and pseudodrusen, including advancing age and smoking (Zhou *et al.,* 2016). Genetic variants including CFH, ARMS2 and HTRA1 increase the risk of reticular pseudodrusen formation, however no genetic factor has been found to predispose to reticular pseudodrusen independent of those that carry risks for AMD (Zhou *et al.,* 2016).

Drusen are thought to result from a combination of the failure to clear debris in the RPE with a local chronic inflammatory response due to complement activated microglia recruited to the site of the debris (Bird, 1992, Khan *et al.,* 2016). Bruch's membrane serves as a semipermeable membrane facilitating the movement of nutrients and metabolites between the outer retina and choriocapillaris. Therefore, drusen accumulation impairs this transport as nutrients must traverse drusen before the flux reaches the retina which leads to RPE and photoreceptor damage (Khan *et al.,* 2016, Stefansson *et al.,* 2011).

1.9. Circadian Rhythms and the iBRB

The role of the sleep-wake cycle and the effect that it has on iBRB physiology is an essential aspect of our research. Aging leads to changes in circadian rhythm and suprachiasmatic nucleus functioning especially in those with aging-associated degenerative conditions and may be a risk factor for the development of diseases in this cohort (Fanjul-moles *et al.,* 2015, Vallee *et al.,* 2020). The circadian clock is a timekeeper that adapts body physiology to diurnal cycles of about 24 hours, enabling individuals to anticipate changes in the environment and adapt appropriately. The circadian clock influences a wide range of processes including sleep-wake transitions, feeding and fasting patterns, body temperature and hormone regulation (Dierickx *et al.,* 2018, Fanjul-Moles *et al.,* 2015). The master clock is located in the suprachiasmic nucleus (SCN) in the hypothalamus. Light is transmitted from the retina to the SCN via melanopsin-expressing intrinsically photosensitive retinal ganglion cells (Kofuji *et al.,* 2016). Neural and hormonal factors such as melatonin and glucocorticoids transmitted from the SCN synchronizes the peripheral clock in all organs to entrain them to the diurnal clock (Dierickx *et al.,* 2018). Light is the most prevalent cue that entrains the circadian clock, but other cues include temperature, nutrition and social interactions (Fanjul-Moles *et al.,*

2015). On a molecular level, the circadian clock is composed of a negative feedback loop of interacting genes that regulate their own transcription/ translation over a 24-hour period (Hood and Amir, 2017). BMAL1 and CLOCK the two core clock transcription factors form a heterodimer that binds rhythmically to enhancer boxes (E-boxes) in the promoters of the negative regulators *Period* (*Per*) and *Cryptochrome* (*Cry*). Following transcriptional induction of *Per* and *Cry*, PER and CRY proteins accumulate and dimerise in the cytosol where they are either degraded or establish an oscillating feedback loop by migrating to the nucleus to suppress the transcription of *Bmal1* and *Clock* (Dierickx *et al.,* 2018). The second BMAL1: CLOCK-dependent feedback loop is driven by rhythmic *Ror* and *Rev-erb* transcription, their respective proteins accumulate and activate or repress *Bmal1* transcription (Dierickx *et al*., 2018). Aging leads to core clock component dysregulation.

The secretion of a range of hormones including melatonin and cortisol is under the control of the circadian rhythm (Pan and Kastin, 2016). Melatonin is rhythmically produced by photoreceptors daily with a peak at night (Tosini and Menaker*,* 1996). Melatonin is an important antioxidant and participates in a diverse range of functions including sleep, circadian rhythm regulation and immunoregulation. Age-associated changes in day/night rhythm of melatonin production have been identified in the elderly (Fanjul-moles et al 2015). Cortisol release is also under the control of the circadian clock however in contrast to melatonin cortisol levels are higher during the morning. With age cortisol rhythms may be altered including a reduction of amplitude and a phase advance with a peak of earlier in the morning (Hood and Amir, 2017). Similarly, to melatonin the disruption of cortisol rhythm in the elderly may indicate progressive degeneration, however the evidence is mixed (Hood and Amir, 2017).

There are reasons to believe that an impairment in circadian rhythm may affect the incidence and pathogenesis of AMD, particularly in relation to RPE rhythms. As we have discussed phagocytosis of POS is synchronised by circadian rhythms and occurs shortly after sunrise followed by lysosomal mediated clearance. Aging is associated with changes in the rhythmicity of melatonin production which can be a major factor contributing to the balance between phagocytosis and clearance and increased levels of ROS leading to degenerative changes in the retina (Stepicheva *et al*., 2019). In fact, mice that lacked the morning burst in phagocytosis but maintained basal RPE phagocytic activity developed age-related loss of photoreceptor protein and accumulated lipofuscin in the RPE (Nandrot *et al.,* 2004). Furthermore, mice lacking melatonin exhibited a peak of phagocytosis 3 hours earlier and this shift resulted in increased lipofuscin accumulation in the RPE (Laurent *et al.,* 2017). In support of this Rosen *et al.,* 2009 reported that the production of melatonin is decreased in AMD patients in comparison to age-matched controls and Yi *et al.,* 2005 concluded that 3mg of melatonin daily protected the retina and delayed macular degeneration.

The advent of spectral domain OCT (SD OCT) has allowed for precise internal retinal structure and retinal thickness analysis. Although not specific to AMD, several studies have reported diurnal variations in other macular diseases including diabetic macular oedema (DMO) and central retinal vein occlusions (CRVO) (Young-Joon *et al.,* 2011, Gupta *et al.,* 2008, Frank *et al.,* 2004). However, studies investigating the diurnal variation of retinal thickness in healthy participants have provided differing results. Young-Joon e*t al.,* 2011 remarked that there was no difference in macular thickness in the morning and evening using SD-OCT. In contrast Ashraf and Nowroozzadeh 2014 demonstrated that macular thickness and macular volume were greater at 7am than 7pm in the inferior 6mm EDTRS subfield and the nasal 3mm and inferior 6mm subfields respectively, however the changes were close due to the repeatability and resolution of spectral domain OCT. Read *et al.,* 2012 observed that although the total retinal thickness does not exhibit evidence of diurnal variation over the course of the day, a small but significant diurnal variation occurs in the thickness of the foveal outer retinal layers with the most prominent changes in the photoreceptor layers at the foveal centre. Other physiological circadian mediated changes include a significant diurnal change in subfoveal choroidal thickness, with this being thicker at night than during the day. However, this is suspected to be correlated to systolic BP as choroidal blood flow is poorly autoregulated and SBP decreases at night (Usui *et al.,* 2012).

1.9.1. Circadian Mediated Changes in Claudin-5

Looking specifically at the interaction between TJ and circadian rhythms He *et al.,* 2014 demonstrated that chronic sleep restriction resulted in decreased tight junction protein expression of key components like claudin-5 and occludin and increased blood brain barrier (BBB) permeability to sodium fluorescein and biotin tracer molecules. Recently Hudson *et al.,* 2019 demonstrated that the gene CLDN5 which encodes claudin-5, is regulated by BMAL1 and the circadian clock. Claudin-5 transcript levels varied depending on the time of day of tissue collection, with transcript levels being lower in the evening when compared to the morning in all tissues examined (including mouse aorta, lung, heart, white fat, liver, adrenal gland, muscle, brown fat, cerebellum, hypothalamus and brainstem) . Although other TJ components ZO-1 and occludin appeared to cycle depending on the time of day, these did not appear to be circadian in nature. In addition, persistent suppression of claudin-5 expression in mice exposed to a cholesterol-enriched diet induced RPE depigmentation and atrophy. Notably mice lack a cone-rich macula similar to the human retina but persistent targeted suppression of claudin-5 in the macular region of non-human primates also induced aberrant RPE structure. It is essential to

note that claudin-5 is not expressed in the RPE which strongly suggests a passive paracellular diffusion of material from the systemic circulation toward to RPE.

Hudson *et al.,* 2019 also demonstrated that the macula in humans and nonhuman primates is more permeable in the evening than the morning. FFA imaging performed in healthy, young participants aged 18 and 30 years old demonstrated that fluorescein signal was evident and more prolonged in the evening compared to the morning in the same subject. Furthermore, Hudson *et al*., 2019 illustrated that this phenotype was also observed in non-human primates. This demonstrated a size-selective passive diffusion of a systemically injected tracer molecule with movement from the inner retinal vasculature into the retinal parenchyma and diffusion to the outer retina and RPE. This is of particular importance as an inner-retina derived contributor to RPE pathology has not been previously described and may play a role in the pathogenesis of conditions involving the RPE such as AMD. We postulate that age-related aberrant claudin-5 cycling in the human retina may lead to a chronic, size-selective disruption of the iBRB with subsequent accumulation of material in the RPE contributing to drusen formation and subsequent RPE atrophy. We therefore propose a circadian-entrained cycling of the permeability of the inner retinal vasculature as a key contributing factor to a dynamic retinal interstitial kinesis that allows for replenishment of substrate to the photoreceptors and the clearance of material from the neural retina daily. These findings implicate an inner retina-derived component in the early pathophysiological changes observed in AMD. We suggest that restoring the integrity of the iBRB may represent a novel therapeutic target for the prevention and treatment of GA. To continue the clinical portion of this research, we are making a full assessment of circadian iBRB regulation in patients with defined degrees of dry AMD and age-matched controls.

1.10. Project Aims and Objectives

We wish to continue the clinical arm of the project carried out by Hudson *et al.,* 2019 by making a full assessment of circadian iBRB regulation in patients with defined degrees of dry AMD and age-matched controls. We hypothesise that the cycling of the iBRB will cease in AMD participants. In gaining an understanding of circadian regulation of the iBRB in a clinical setting in human subjects, we will be positioned to make profound conclusions on its role in AMD pathophysiology, aiding our understanding of GA pathophysiology and potentially, in the future, development of therapeutic strategies to treat the condition.

The main objectives of this initial investigation are:

- To establish the study methodology including:

- Participant recruitment.
- Safety protocols.
- Data collection.
- AMD grading.
- Results analysis.

With an established study methodology this project will be continued over the coming years by other members of the Campbell Laboratory with the goal of expanding the number of study participants in the current demographic of early mild and early intermediate AMD and extending this to later stages of AMD including GA and CNV.

- Data collection:
  - Collection of fundal photographs, FFA, OCT and autofluorescence (AF) images in the morning and evening in the same individual.
  - Collection of participants' relevant medical history via a participant health questionnaire.
  - Collection of participants' chronotype using the Munich Chronotype Questionnaire (MCTQ).
  - Collection of PBMCs for inflammatory status including IL-beta and IL-18 production.
  - Collection of serum and plasma samples for cortisol, melatonin and S100B levels.
  - Collection of DNA from each participant for AMD variants.

- Results analysis to assess circadian regulation of iBRB integrity in participants with specific grades of AMD (early mild AMD and early moderate AMD) and aged-matched control participants:
  - Quantitative FFA analysis comparing the morning and evening images in the same individual to assess retinal vasculature permeability and integrity.
  - Quantitative OCT analysis of the morning and evening images to assess retinal thickness changes and the presence of drusen and pseudodrusen.
  - Analysis of the MCTQ to determine participants' chronotype and stratify these results within each participant category.

As described above we have collected participants' blood samples at both timepoints however the analysis of these samples is beyond the scope of this current thesis and will be performed as part of the ongoing study. In particular, we will screen these samples to correlate

any potential changes in inflammatory status, melatonin and cortisol levels and circadian mediated changes in clock components with barrier integrity at particular times of day. In addition, participants will have DNA isolated and subsequently genotyped for AMD risk variants such as Complement Factor H (CFH), Complement Factor B (CFB), Age-Related Maculopathy Susceptibility 2(ARMS2)/ High-Temperature Requirement A Serine Peptidase 1 (HTRA1) and Apolipoprotein E (APOE) to determine if there is a link between severity of disease, risk variant and changes in iBRB integrity and vessel permeability. These results will be compared to the results of the same experiment in healthy human controls aged between 18-30 years completed last year.

CHAPTER 2: Methods and Materials

2.1. Ethical Approval

In July 2019 ethical approval was obtained from the Research and Ethics Committee in the Royal Victoria Eye and Ear Hospital (Appendix A). The participant information leaflet, consent form, MCTQ and patient health questionnaire was reviewed by the data protection officer (DPO) and deemed to be GDPR compliant.

2.2. Recruitment

2.2.1. Inclusion and Exclusion Criteria

Inclusion criteria for the AMD group was as follows: male and female individuals of any age with a confirmed diagnosis of early mild or early moderate AMD. AMD severity was graded using the International Classification and Grading System for AMD and is discussed later in this section.

Exclusion criteria for the AMD group was as follows: documented allergy to sodium fluorescein or known shellfish allergy; AMD in early severe or late grade; previous treatment with intravitreal injections of anti-VEGFs for AMD, diabetic macular oedema (DMO), and retinal vein/ artery occlusions; history of uncontrolled ocular conditions including glaucoma and proliferative diabetic retinopathy; recent ocular surgery of any kind on test eye within 3 months of investigations; recent surgery under general anaesthetic within 3 months of investigations; known inherited retinal dystrophy; previous retinal detachment.

Inclusion criteria for the control group was as follows: male and female participants >65 years of age or aged <65 and age matched to a specific participant in the AMD group.

Exclusion criteria for the control group was as follows: documented allergy to sodium fluorescein or known shellfish allergy; previous diagnosis of AMD of any grade; previous treatment with intravitreal injections of anti-VEGFs for AMD, DMO, and retinal vein/ artery occlusions; history of uncontrolled ocular conditions including glaucoma and proliferative diabetic retinopathy; recent ocular surgery of any kind on test eye within 3 months of investigations; recent surgery under general anaesthetic within 3 months of investigations known inherited retinal dystrophy; previous retinal detachment.

2.2.2. Target recruitment numbers

As this is a pilot study, we do not have previous studies to base our recruitment numbers on however based on power analysis we have established 100 participants with early/ early moderate and 100 control participants as a target number to recruit for the duration of the

study. It should be noted that this study will continue on over the course of several years with new research fellow overseeing the study. For this reason, we have accepted that the numbers required would not be obtainable over the course of one year and the main focus for the primary year of this study is to put structures in place and to establish recruitment and testing protocols. A target number of 20 participants in the AMD group and 15 control participants was established for the first year of the study.

2.2.3. The recruitment process

We identified two principle methods of recruitment for our study; recruitment of members of the public through promoting our research online and recruitment of patients through the hospital and outpatient setting.

In order to publicise our study and make information regarding the recruitment process available to members of the public we entitled our project the Irish Retinal Circadian Project (IRCP) (Figure 2.1). We have built a website (www.circadianretina.com) in order to make information regarding the project and contact details of the research team available. The website also acted as a platform to post about publications in scientific journals relevant to the research or articles written about the study along with documenting our participation in upcoming or past conferences. The website facilitated participants interested in taking part in the study to learn more or those who have already taken part to stay up to date with our progress. The website was built and maintained using WordPress software. A twitter account (@circadianretina) was created in order to engage with other researchers and groups involved in ophthalmology in Ireland. We devised a study information leaflet which included study objective and description, eligibility criteria and discussed what taking part in the study would involve.

Figure 2.1. The logo for The Irish Retinal Circadian Project (IRCP)

Fighting Blindness is an Irish patient-led charity with a wealth of knowledge regarding research in the field of ophthalmology and established connections with individuals living with sight loss and their families. Fighting Blindness regularly reaches out to members via mailing lists and Facebook groups, and regularly posts on their website and on Twitter about ongoing research projects, publications and conferences that their members may be interested in. In August 2019 we contacted Dr Laura Brady, Head of Research in Fighting Blindness and with Dr Brady's assistance our information leaflet and call for applicants was disseminated through Fighting Blindness's social media accounts, mailing lists and published on their website. Through this call for applicants we recruited individuals with AMD and control participants.

We also recruited participants from Mr Cahill's outpatient clinics in both The Royal Victoria Eye and Ear Hospital and Progressive Vision, a private ophthalmology clinic in The Beacon Hospital, Dublin. Progressive Vision uses electronic patient records (EPR) to manage their patient information, clinic scheduling and clinical management. There are two main systems of EPR in use in Progressive Vision; Medisoft (*Medisoft Ltd, UK)* can record clinic visits, assessments, investigations and ophthalmic procedures and Acuitas (*Ocuco Ltd, Ireland)* allows users to manage workflows, diary, examinations and SMS reminders.

Both patients with early and early-intermediate AMD and age-matched controls were recruited from Progressive Vision. When patients who met the selection criteria attended Progressive Vision for their routine clinic appointment, the research was briefly discussed with them by an ophthalmologist or optometrist and they were asked if they would like to be contacted by one of the members of the research team to learn more about participating in the study. Post-operative cataract patients attending for routine follow up appointments were recruited as age-matched control participants.

2.3. Public and patient participation

There is a growing acknowledgement of the importance of involving the public in research. INVOLVE (2012) defines public involvement in research as research being carried out 'with' or 'by' members of the public rather than 'to', 'about' or 'for' them. We wished to promote public and patient involvement (PPI) in our research project as early as possible as we felt this would help to provide a different perspective, especially considering individuals' personal knowledge and experience with AMD. Public involvement offers unique insights and allows us to build and strengthen the relevance, transparency and ethics of our research and give us invaluable advice around encouraging participation in our study. We met with the Macular Impairment Support and Togetherness (MIST) group who are an Irish support group for those with loss of central vision. The MIST group is composed of those with AMD and

people who have family members with the condition; they meet several times a year and welcome guest speakers with experience or interest in AMD to run talks with the group. We have facilitated the MIST group to hold their meetings in the Smurfit Institute of Genetics and in the past have given talks to the group to discuss our research to them. Furthermore, in order to ensure that our methods, leaflets and questionnaires are sensitive to each participant's situations we ensure that we contact each participant following the study in order to see feedback and implement this going forward.

2.4. Testing procedures

Investigations were carried out initially in Progressive Vision for n=14 and in The Royal Victoria Eye and Ear Hospital for the remaining participants (n=13). It should be noted that all investigations were uniform in both locations. The below sections document the procured carried out in the order that they were carried out at each testing session.

2.4.1. Informed consent

Following the recruitment of participants, a member of the research team contacted them over the phone to discuss the project in depth and questions regarding the research. Potential participants were informed that the study was voluntary, and they would be able to withdraw the participation at any stage during the course of the study. After this phone call an email was sent to the participant documenting the information discussed over the phone and a participant information leaflet was attached to this email.

On the day of the study participants were again informed of the testing procedure, allowed to have all their questions answered to their satisfaction and were again informed that the study was voluntary, and they could withdraw consent at any point. Written informed consent was obtained from every participant prior to their involvement by a medically qualified designee. All research participants were deemed to have capacity to give informed consent.

2.4.2. Munich Chronotype Questionnaire

We used the MCTQ (see Appendix A) to assess participants' chronotype. A chronotype is defined as an individual's sleep-wake time preferences based on their circadian rhythm (Ryu *et al.,* 2018). Children generally have earlier chronotypes, progressively becoming later during development, reaching a maximum lateness around the age of 20 and then becoming earlier again with increasing age (Ronneberg *et al.,* 2007). The MCTQ

estimates chronotype by measuring actual sleep timing, distinguishing between work and free days and it has been extensively used over the past 15 years across many different fields of research. The MCTQ uses the midpoint between sleep onset and offset on free days (mid sleep on free days MSF) to assess chronotype. The midpoint of sleep has been found to be one of the most accurate behavioural markers for circadian phase (Terman *et al.,* 2001). MCTQ parameters are MSW (mid sleep on weekdays), mid-sleep on free days (MSF) and mid-sleep on free days corrected for sleep debt on weekdays (MSFsc). The MCTQ uses MSFsc as a chronotype indicator with high MSFsc reflecting stronger eveningness tendency (Ronneberg *et al.,* 2019).

Other methods of evaluating chronotype include the Morningness Eveningness Questionnaire (MEQ), and physiological measurements such as Dim Light Melatonin Onset (DMLO) and polysomnography. The MEQ asks questions with Likert-type responses based on sleep preferences to determine a tendency towards morning-type, evening-type or intermediate type. However, the MEQ scores are inconsistent across younger and older age groups and also across different populations (Levandovski *et al.,* 2013). DLMO is a physiological tool that may provide more biologically accurate info but are time-consuming and costly. The benefits of the MCTQ over these other methods are that it provides a quick, cost-effective and accurate way of measuring circadian features that have been correlated with several aspects of human health and performance. Ryu *et al* 2018 supported the validity of MCTQ in older adults, demonstrating that the MSFsc using MCTQ was significantly positively correlated with MSFsc using sleep diary and actigraphy. The limitations of the MCTQ are that all calculations rely on structured work schedules asking about work days and work free days, which may hinder its use in our population. Feedback from our participants regarding the MCTQ documented difficulties completing the MCTQ following retirement of without a structured work week. We addressed this by asking participants to only fill out the free day section if they did not work regularly.

2.4.3. Participant Health Questionnaire

To accompany the MCTQ we devised a participant health questionnaire to gather information about participants' past ocular history, past medical and surgical history, medications, allergies, family history, smoking history and ethnicity. The questionnaire was collected using an anonymised online form which automatically inputted to a password protected spreadsheet. Only the members of the research team had access to this spreadsheet. For safety the form was always completed prior to the investigations either by the participant at

home prior to coming in for testing or along with one of the research team on the day of the study.

2.4.4. Measurement of Visual Acuity

Visual acuity (VA) is related to the angle subtended at the eye by the smallest recognizable optotype (figure or letter of different sizes) and is measured by the patient's ability to identify progressively smaller optotypes (Hussain *et al*., 2006). VA was measured for all participants at both the morning and evening visit using the Snellen chart. Snellen charts were projected onto a screen 6m from participants and one eye was occluded at a time. Vision with and without pinholing was obtained and best corrected visual acuity (BCVA) was documented for each individual. The Snellen chart is the most widely adopted tool for measuring VA and was chosen for this study as it is the standard VA test used in both the Royal Victoria Eye and Ear Hospital and Progressive Vision and was readily available in these sites. Each letter on the Snellen chart subtends an angle of 5min of arc at the appropriate distance and each separate part of the letter subtends an angle of arm of 1 min of arc. 'Standard vision' is the ability to recognise an optotype at a visual angle of 1 minute of arc. People with normal vision are able to read the 6-metre line at 6 metres *i.e.* 6/6 vision. Although Snellen charts are widely used they have several well documented limitations: firstly there is inconsistent progression in letter size between lines; secondly the letters used on the chart are not equally legible; thirdly the spacing between letters and rows is unequal and finally there are large gaps between acuity levels at the lower end of the chart (Falkenstein *et al.,* 2008).

The ETDRS chart is a logMAR based chart and is currently considered the gold standard test for measuring and monitoring VA in AMD patients (Chew *et al.,* 2011). LogMAR VA measurements are viewed to be more precise and reliable than Snellen VA measurements in those with both good and poor vision ranges (Bokinni *et al.,* 2015). There are difficulties in introducing and employing logMAR based acuity measures as they take twice the time to read and there can be difficulties in standardising testing procedures and scoring methods. The technique for measuring VA using a logMAR chart is similar to that of the Snellen chart however the test distance is 4 metres. In contrast to the Snellen chart the ETDRS chart employs regular geometric progression of the size and spacing of the letters following a logarithmic scale in steps of 0.1 log units, equal numbers of letters in each row and comparable legibility of the letters used (Falkenstein *et al*., 2008). The ETDRS measurements also yielded a better VA particularly in participants with vision <20/200 (representing advanced AMD) (Falkenstein *et al.,* 2008) and gave less variability in results. For these reasons, researchers continuing this study should consider employing the ETDRS chart for assessing VA instead of

the Snellen chart. For assessment and comparison of visual acuity we converted participant's Snellen Visual Acuity into an ETDRS equivalent using NHS guidelines. In the event of a change from the use of the Snellen Visual Acuity chart to the ETDRS chart the data collected to date would still be usable with the conversion applied however the different methods of assessing VA should be noted.

2.4.5. Measurement of Intraocular Pressure

All participants had their intraocular pressure (IOP) measured in both eyes at their morning and evening visits using a Goldmann applanation tonometer (GAT) mounted on a slit lamp. The GAT is considered the gold standard instrument for measuring IOP. A drop containing a combination of proxymetacaine hydrochloride 0.5% w/v and fluorescein sodium 0.25% w/v was applied to each eye. Of note if the participants' IOP was >25mmHg their central corneal thickness was measured using a pachymeter and adjustments to IOP were made based on the central corneal thickness. If a participants' IOP was still >25mmHg then their pupils were not dilated, and they would not take part in the study on that occasion.

2.4.6. Methods of Pupil Dilation

Following the measurement of intraocular pressure participants' pupils were dilated using 1 drop of 1% tropicamide eye drops administered under the lower eyelid. Sufficient time was allowed for the pupils to dilate fully. On the first visit both pupils were dilated to allow for fundal photography in both eyes, on the second visit only the test eye was dilated.

2.4.7. Peripheral Venous Sampling

A 22-gauge cannula was inserted in either the antecubital fossa or the dorsum of the hand and peripheral blood samples were drawn from this at both the morning and evening visits. A yellow serum separating vacutainer containing silica particles and a serum separating gel was used to measure cortisol and melatonin, this sample was kept on ice following collection until analysis in the laboratory. Two purple ethylenediaminetetraacetic acid (EDTA) vacutainers were used for peripheral blood mononuclear cell isolation (PBMC), the EDTA acts as a potent anticoagulant binding to calcium in the blood. One PAXgene blood RNA tube was used to stabilise and collect intracellular RNA.

2.4.8. Fundal Photography and Grading

Fundal images were acquired through participants' dilated pupils and were taken of both eyes on the first visit. Images were acquired using a Topcon 50ex in Progressive Vision and a Topcon 50x in The Royal Victoria Eye and Ear Hospital. Three images were taken on each eye, a colour fundal image centered on the macula, a colour fundal image centered on the optic disc and a red free fundal picture centred on the macula. These images were used to grade participants' AMD severity or to confirm there were no signs of AMD present in control subjects.

The grading system used was the modified version of the International Classification and Grading system for AMD (Bird *et al*., 1995), with the ARM category replaced with three categories of early AMD (as was used by Connolly *et al.,* 2018, Figure 2.3).

Participants were defined as follows:

Category 1: no disease (free of age-related macular abnormalities)

Category 2: early mild AMD (>10 hard drusen <63 μm)

Category 3: early moderate AMD (at least one soft druse >125μm)

Category 4: early severe AMD (soft drusen and hyperpigmentation)

Category 5: late, choroidal neovascularisation

Category 6: late, geographic atrophy

Category 7: late, mixed choroidal neovascularisation and geographic atrophy

The final grade for each patient is based on the worst eye in terms of severity. Following this we devised a grading form on an excel spreadsheet which documents image focus/ clarity, the presence and size of drusen, the presence of hyperpigmentation and hypopigmentation, and the presence of geographic atrophy in each eye.

2.4.9. Optical Coherence Tomography and Fundus Autofluorescence Imaging Acquisition

Following the acquisition of fundal images one eye was designated the test eye; in control participants and participants with an equal grade of AMD in both eyes the test eye was selected at random and in those with different grades of AMD in each eye the eye with the either early mild or early intermediate AMD was selected. Spectral Domain optical coherence tomography (SD-OCT) images of the retina centered on the macula were taken in the test eye

of each participant at both AM and PM visits using the Heidelberg Spectralis (*Heidelberg Engineering, Heidelberg, Germany*). A fundus autofluorescence (FAF) image was also taken of the participant's test eye using the Heidelberg Spectralis (*Heidelberg Engineering, Heidelberg, Germany*).

2.4.10. Fundus Fluorescein Angiography Acquisition

Fundus fluorescein angiography (FFA) images were captured with a 30° angle of viewing using the Heidelberg Spectralis (*Heidelberg Engineering, Heidelberg, Germany*). These were captured at both timepoints with a minimum of 48hours between visits to allow for fluorescein to be renally excreted. 2ml of sodium fluorescein 20% w/v (400mg) was injected intravenously by a medical doctor through a 22-gauge cannula followed by a 5ml flush of normal saline. Each participant was given the same dose of sodium fluorescein and each individual had the cannula sited at the same location for the AM and PM visit in order to ensure uniform time for fluorescein to travel from arm to eye. Immediately following the fluorescein administration angiography images were captured at regular intervals up to 10 minutes. There is a protocol in place in the event of anaphylaxis in the Royal Victoria Eye and Ear Hospital and IM adrenaline, IV hydrocortisone and PO antihistamines are all readily available in the room where the investigations were taking place.

2.5. Result Analysis

2.5.1. Optical Coherence Tomography Analysis

OCT images were analysed for retinal thickness at each area as designated by the ETDRS grid (Figure 2.5.1.) using technology on the Heidelberg Spectralis. These were aggregated and plotted using Prism. OCT images were also assessed for changes in the ellipsoid layer on OCT the presence of reticular pseudodrusen and the presence of hyperreflective crystalline deposits, all of which are associated with a worse prognosis in AMD (Filho *et al.,* 2015, Sivaprasad *et al.,* 2016, Wightman and Guymer 2019, Fragiotta *et al.,* 2019).

Figure 2.5.1. ETDRS grid over the human macula. The regions consist of the central fovea (1), inner macula (2) and outer macula (3).

2.5.2. Manual Fundus Fluorescein Angiography Analysis

The macula was divided into 3 regions based on the ETDRS grid, comprising (1) central fovea, (2) inner macula, and (3) outer macula (Figure 2.5.1.). Images were analysed using ImageJ technology. A circle corresponding to the area of the central fovea (0.58 pixel diameter), inner macula (1.72 pixel diameter) and outer macula (3.52 pixel diameter) respectively was drawn on each image based on an estimate of central foveal location (Figure 2.5.2.). These three areas were manually mapped at every time frame for each participant using blood vessels as reference points to ensure the same the location was standard across all images. The raw intensity value of each area was calculated using the measure function on ImageJ and multiplying the intensity density by the mean area. In order to control for difference in overall light intensity between images we measured the raw intensity at three defined points along a blood vessel at each time point, averaged this value and divided the overall raw intensity value of each time point by the average blood vessel raw intensity value at the corresponding time point. Following this time defined time points were set to 100% (2 mins, 3mins, 4mins, 5mins, 6mins, 7 mins, 8mins, 9mins, 10mins) to allow for comparison. The results were plotted on Prism.

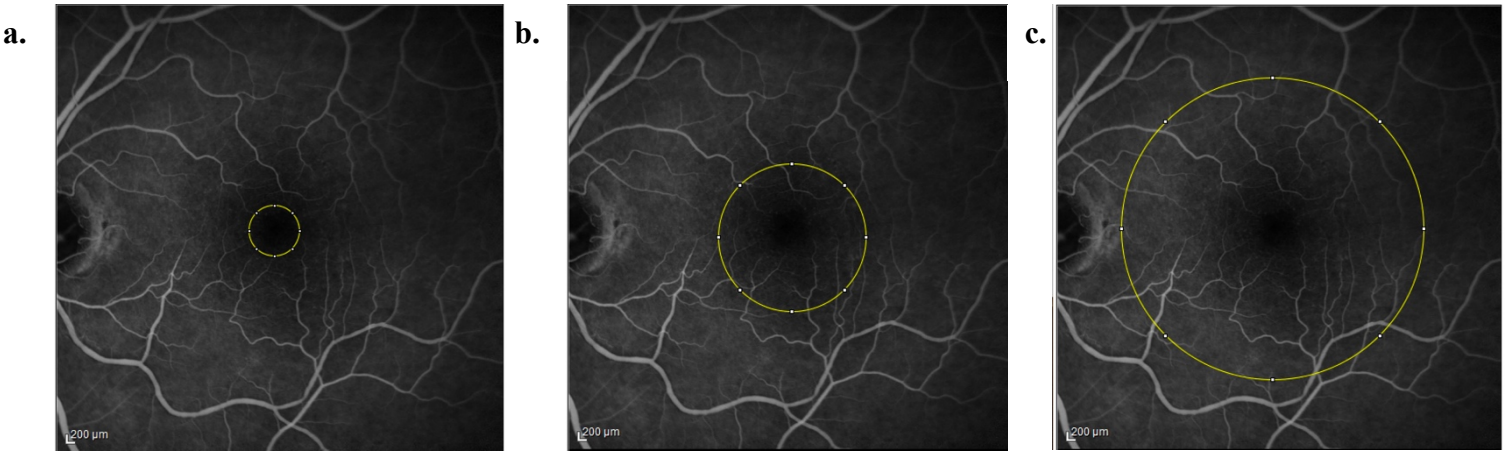

Figure 2.5.2. An FFA image taken from a participant at the 5-minute time frame with circle the circle in **a.** corresponding to the central fovea (diameter of 0.58 pixels), the circle in **b.** corresponding to the inner macula (diameter of 1.72 pixels) and the circle in **c.** corresponding to the outer macula (diameter of 3.52 pixels).

2.5.3. Automated Fundus Fluorescein Angiography Analysis

In order to standardise image analysis and to ensure repeatability and accuracy of FFA quantification an app was developed to process and analyse the FFA image data without needing code. This app was developed by Dr Jeffery O'Callaghan in the Campbell Laboratory. This FFA software was initially used to analyse the FFA data collected by the Campbell Laboratory in non-human primates (NHP) and in healthy young volunteers ages 18-30 as presented Hudson *et al.,* 2019 to allow for comparison between the manual analysis.

The image processing workflow proceeds as follows: first it identifies and sorts images, extracts timepoints from the filename, crops/ flips and light corrects images where applicable, creates a montage/ tiff stack, registers images, defines macula and/ or reference vessels, applies the ETDRS grid, calculates the mean intensity and area, calculates the integrated grey level, quality controls for problematic cases and detects outliers. Initially a code was written in MATLAB using the MATLAB App Designer to develop the graphical user interface (GUI) (Figure 2.5.3.1.).

In order to process the images the app creates an image stack converts the image to greyscale, extracts the timepoint from the file name, converts the minutes and seconds to decimal format, crops the image, applies illumination correction (if specified in the GUI), flips the image horizontally if the folder ends with OD, appends the images to a tiff stack, saves the stack, creates the montage and saves this and finally clears large variables to save memory. There is a section for reference vessel data which creates a maximum intensity projection

(MIP), if the “define macula” box is ticked on the GUI the user can double click the centre of the macula on the MIP. The code takes this coordinate and uses it as the centre point for the ETDRS grid. If it is not ticked then it assumes the middle of the picture is the macula centre. If reference vessel is ticked, a message box tells the user to click 3 points for a reference vessel. It takes these coordinates and uses it for normalisation later. The “generate region of interest (ROIs)” section assigns the macula centre from “define macula” and formulates different radii for the ETDRS grid. It then makes a mask for each of the 5 combinations of regions so that only the region of interest is considered.

Data is generated in the “data collection” section. The regionprops function is used to apply the mask to each image from the stack and subsequently calculates the mean intensity and area. These two values are then multiplied to produce the integrated grey level (IGL). If the reference vessel is selected, then it will also divide the IGL by the average reference value for that image. There is an IGL value created for each ROI for each image in every subfolder. A remove outliers code looks at all data for participants and decides if any AM or PM data is an outlier (defined at being outside a 10^{th} percentile). If anything is found to be below this it will be removed from the dataset. All of the remaining data, names, timepoints and key info is saves to a .mat file in the folder for analyses.

The analyse function takes all the data in the .mat file and generates figures and statistics. Firstly, the user is asked to select the folder of data to analyse. Under “choose graphs” it determines which graphs to plot based on the values that were selected in the GUI. The “define timepoints” section allows the user to define the phases of the FFA images. This allows the user to specify which time points correspond to early phase or to mid phase and adjust if needed. The “normality test” section puts all of the data in to one vector in order to perform a normality test using the Anderson Darling test. This then plots a probability plot and histogram of the data, saves this and puts it on the app. Next, based on the results of the Anderson Darling test the software determines whether the data is from a normal distribution or not and sets the statistical methods and measures of central tendency for all of the following analyses. The “IGL vs time” section formulates graphs for each participant plotting IGL over time for AM and PM. The “cumulative intensity” sums the data for each region of interest and creates a boxplot. It also makes a boxplot for the percentage difference between sum PM and sum AM data. These figures are initialised, plotted and saved. Statistics are performed and data is appended to the table. Similarly, for the phases graphs, the required data is extracted using the timepoint indices and plotted. Again, the figure is posted to the app, saved to the folder and statistics are performed and appended to the table. The “rates of change” takes a line of best fit of the data within a phase, determines the slope and compares AM to PM statistically. Finally, the table is

saved to excel, all figures are closed and the info panel on the app will indicate that the analysis is complete.

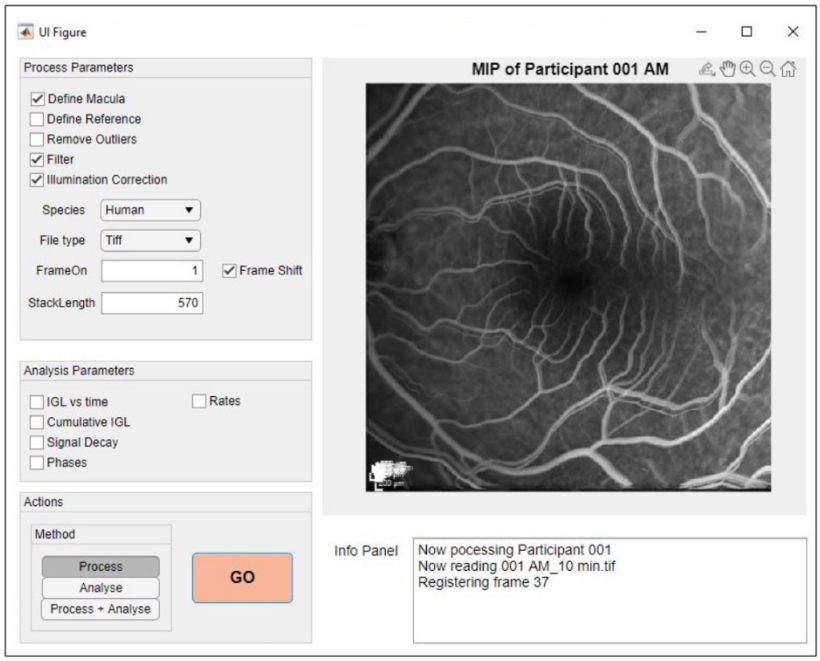

Figure 2.5.3.1. Example of the graphical user interface (GUI) of the FFA quantification app.

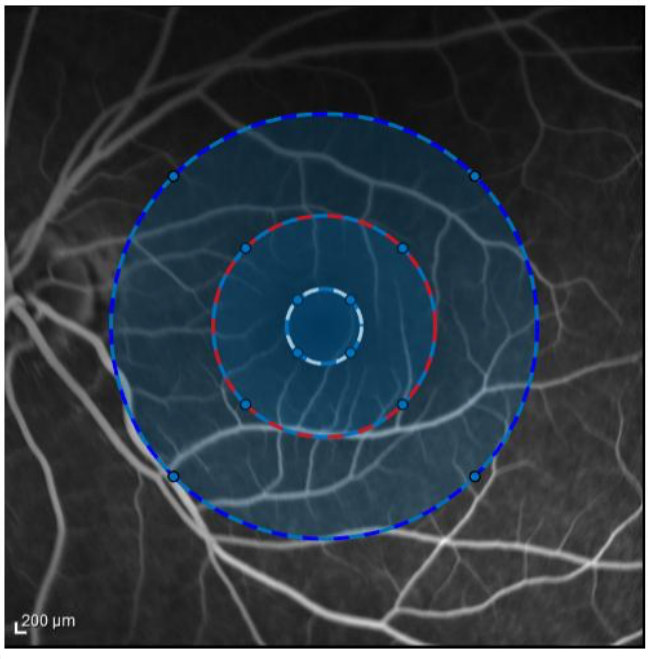

Figure 2.5.3.2. An FFA image with the ETDRS grid applied by the FFA quantification app.

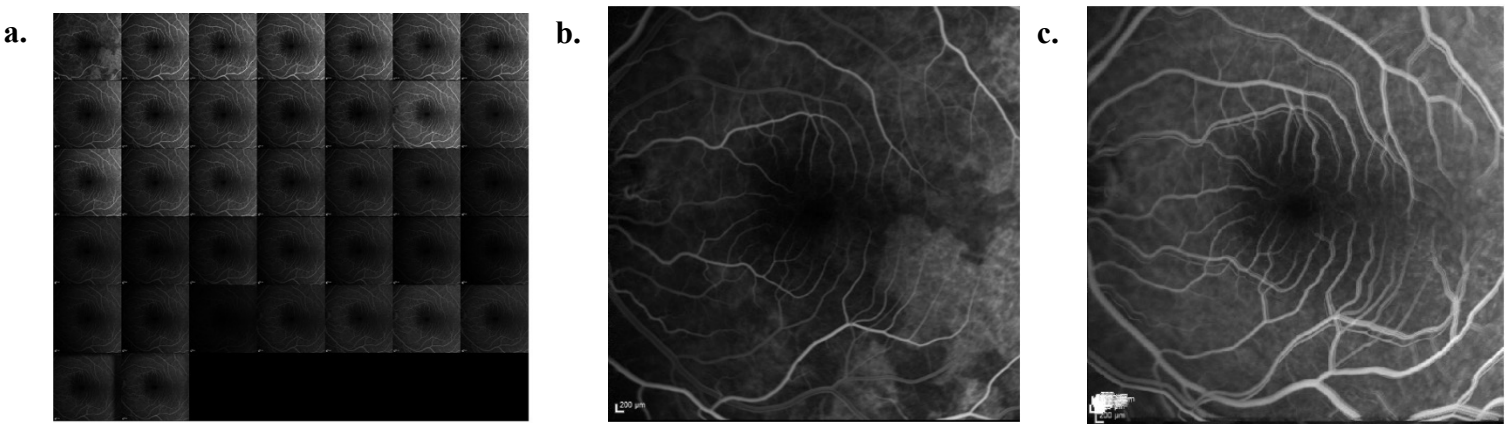

Figure 2.5.3.3. Sample images from the processing workflow. Image **a.** demonstrates a montage being created for a selected participant, image **b.** is a Tiff and registered stack and image **c.** is the maximum intensity projection for the same participant.

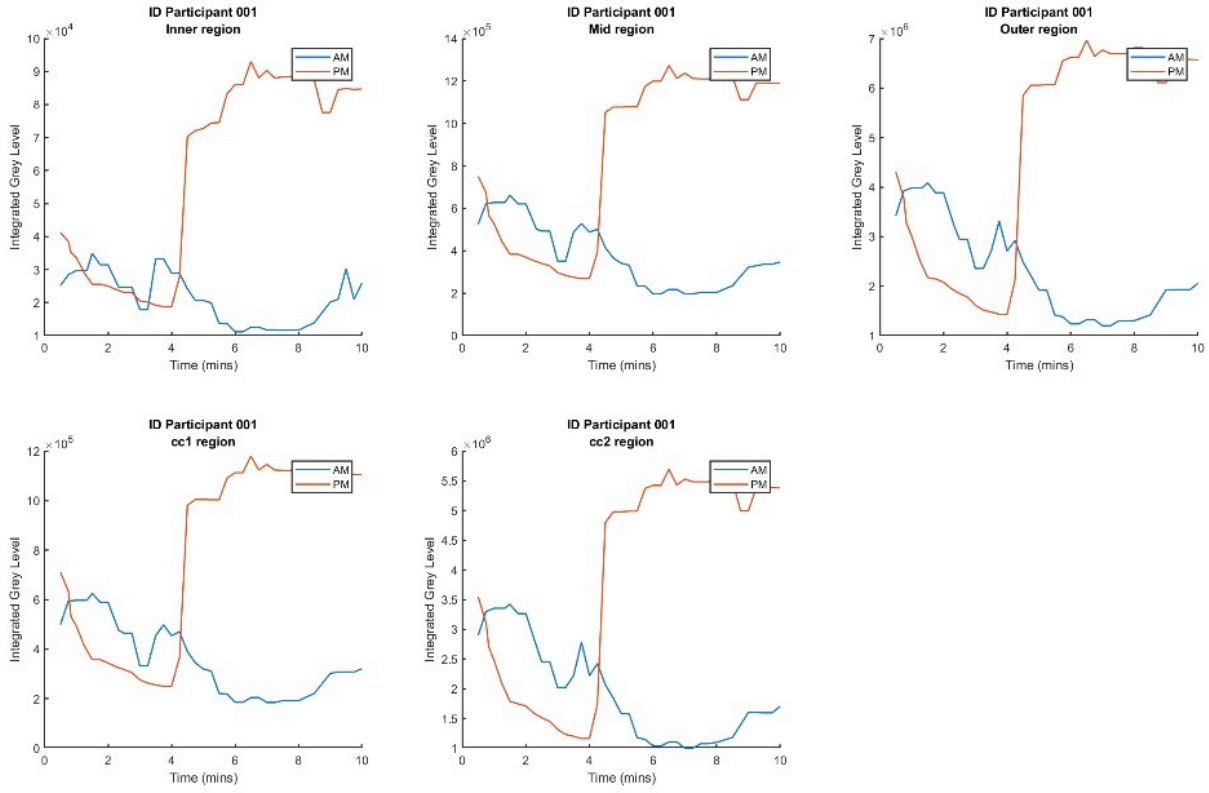

Figure 2.5.3.4. Example of a graph produced for each region of the ETDRS grid using the FFA quantification software on a participant in the AMD cohort. Traces show the IGL (interpreted as the sum intensity) at each timepoint for one participant in the inner region, mid region, outer region, cc1 (inner and mid region) and cc2 (all three regions).

2.5.4. Blood Sample Analysis

A peripheral venous sample was drawn from each participant at both the morning and evening visits to correlate any potential changes in inflammatory status, melatonin and cortisol levels and circadian mediated changes in clock components with barrier integrity at particular times of day. In addition, participants will have DNA isolated and subsequently genotyped for AMD risk variants to determine if there is a link between severity of disease, risk variant and changes in iBRB integrity and vessel permeability. Of note this analysis was carried out by another member of the Campbell Laboratory so will only be discussed briefly in this section.

Serum and plasma samples were screened for cortisol and melatonin using ELISA analysis as per the Campbell Laboratory's ELISA protocol. Peripheral blood mononuclear cells (PBMCs) were isolated and screened for inflammatory markers including IL-1beta and IL-18. RNAseq was performed to determine the levels of clock components BMAL-1, Per2 and Rev-Erb alpha. Genotyping will be performed for known AMD risk variants associated with AMD including Complement Factor H (CFH), Complement Factor B (CFB), Age-Related Maculopathy Susceptibility 2(ARMS2)/ High-Temperature Requirement A Serine Peptidase 1 (HTRA1) and Apolipoprotein E (APOE). This has not yet been performed but will be carried out once more participants have been recruited. This will determine if there is a link between severity of disease, risk variant and changes in iBRB integrity and vessel permeability.

CHAPTER 3: Results

3.1. Participant Demographics

	Category 1 (n=9)	Category 2 (n=6)	Category 3 (n=11)	Category 6 (n=1)
Gender				
Male	n=6	n=1	n=1	n=1
Female	n=3	n=5	n=10	
Age				
Average	72.4	75.0	72.7	78.0
Standard deviation	6.8	5.7	7.1	
Height				
Average	169.9	161.7	165.4	180.0
Standard deviation	9.6	8.9	6.7	
Weight				
Average	82.2	72.3	66.9	79.0
Standard deviation	21.6	8.9	9.2	
Ethnicity				
Caucasian (% of category)	100,00 %	100,00 %	100,00 %	100,00 %

Table 3.1.1. Table demonstrating the gender, age, height, weight and ethnicity breakdown across the control group (category 1) and the three grades of AMD (category 2, category 3 and category 6) participants.

In total 27 participants were recruited to take part over the first year of the study. Efforts were made to age match and gender match each category (as represented in Table 3.1.1.). Of note, a larger number of female participants were recruited in the early mild and early intermediate categories. This reflects the numbers of eligible participants that were interested in taking part in the study. We intend going forward to recruit more male participants in these categories. It should also be noted that all the participants involved in the study were Caucasian, again as the study numbers expand further, we intend to recruit participants of other ethnicities.

	Category 1 (n=9)		Category 2 (n=6)		Category 3 (n=11)		Category 6 (n=1)	
	AM	**PM**	**AM**	**PM**	**AM**	**PM**	**AM**	**PM**
OD (LogMAR)								
Average	-0.03	0.09	0.03	0.00	0.10	0.11	0.12	0.22
Standard deviation	0.08	0.10	0.09	0.09	0.10	0.11		
OS (LogMAR)								
Average	0.03	0.02	0.03	0.04	0.09	0.11	CF	CF
Standard deviation	0.21	0.22	0.09	0.08	0.07	0.08		

Table 3.1.2. Table representing the visual acuity (VA) in LogMAR values in each AMD grade. Of note the VA was measured using a Snellen chart and converted to LogMAR equivalent using the NHS conversion scale (see APPENDIX A). A LogMAR value of 0,00 equates to 6/6 Snellen equivalent and negative values represent VA greater than a 6/6. CF= count fingers.

	Category 1 (n=9)			Category 2 (n=6)			Category 3 (n=11)			Category 6 (n=1)		
	AM	**PM**	**% IOP change**	**AM**	**PM**	**% IOP change**	**AM**	**PM**	**% IOP change**	**AM**	**PM**	**% IOP change**
OD (mmHg)												
Average	14.44	14,67	-1.54 %	15.00	14.83	0.90 %	14.36	13.00	13.21 %	10.00	15.00	
Standard deviation	2.40	0,87	-13.87 %	2.45	1.72	10.04 %	2.54	2.76	20.34 %			
OS (mmHg)												
Average	15.22 2	14.67	3.56 %	15.17	15.17	-0.35 %	15.20	14.73	4.80 %	10.00	15.00	
Standard deviation	2.17	1.23	8.62 %	2.71	2.14	6.90 %	4.94	4.74	11.28 %			

Table 3.1.3. Table representing intraocular pressure (IOP) measurements in the right eye (OD) and left eye (OS) at the AM and PM visit in each participant demographic. The percentage difference of IOP was measured comparing AM values with PM values.

The visual acuity in each group is shown in Table 3.1.2; in Category 2 and 3 the participants visual acuity is well preserved as we would expect to see in those with early mild and early intermediate AMD. The participant in Category 6 is count fingers (CF) in the left eye secondary to the progression of GA atrophy with foveal involvement in this eye, of note the eye with the better visual acuity was tested.

The normal IOP range is between 12-21 mmHg; all of the participant's IOP measurements were below the upper limit of normal. There was no remarkable change in IOP measurements between the AM and PM visit across the categories, this is unusual as IOP is known to demonstrate diurnal variation (Mansouri *et al.,* 2020). IOP fluctuations range from 2mmHg to 6mmHg non-glaucomatous eyes, however it should be noted that many studies regarding circadian mediated IOP fluctuations focus primarily on patients with glaucoma where the fluctuations are significantly greater and may be more than 10mmHg (Drance *et al.,* 1963, Agnifilli *et al.,* 2014). We would expect to observe higher IOP measurements in our participants in the morning due to a nocturnal IOP rise (Mansouri *et al.,* 2020). IOP peaks during and gradually decreases during the morning, reading the lowest value in the early afternoon (Agnifilli *et al.,* 2014). Despite this, Agnifilli *et al.,* 2014 also demonstrated that in healthy subjects no significant differences were found when comparing IOP in the morning with the afternoon-evening period, whereas patterns significantly differed when comparing the morning with the night which would be in keeping with our results. However , it should be noted that body position adds a possible bias to IOP measurements which is discussed at length by Mansouri *et al.*, 2020. A combination of hydrostatic changes and an elevation of episcleral venous pressure when the body is supine contributes to a consistent IOP elevation (Mansouri *et al.*, 2020). This means that a supine body position during sleep causes an increased IOP at night. Consequently the positioning of the patient when measuring IOP plays an important role. When IOP is measured in the habitual positions (sitting during the day and supine at night) the IOP is highest at night whereas in some studies when IOP is measuring in the sitting position at all timepoints the IOP is often lower at night than during the day (Mansouri *et al.,* 2020). For our study IOP was measured with participants sitting at both time points and as they had to travel from home to the hospital for testing they were generally prone for at least an hour before their IOP was measured which may account for the similar IOP measurements. Another possible explanation for the IOP measurements being similar in the morning an evening may be that the study numbers were too low to detect a difference between the morning and evening IOP values

	Category 1 (n=9)	Category 2 (n=6)	Category 3 (n=11)	Category 6 (n=1)
MSFsc (hours)				
Average	3,653	3,896	3,571	5,168
Standard dev	0,905	0,946	0,921	
AM time post-MSFsc (hours)				
Ave	4,036	3,752	4,200	2,499
Std Dev	1,095	1,119	0,946	
PM time pre-MSFsc (hours)				
Ave	7,883	8,309	7,821	8,785
Standard dev	0,725	0,771	0,893	

Table 3.1.4. Table representing the mid-sleep time on free days corrected for sleep debt on weekdays (MSFsc), the AM test time following MSFsc and the PM test time prior to MSFsc in each category as measured using the Munich Chronotype Questionnaire (MCTQ).

The MCTQ was used to calculate participants chronotype, with larger values representing a later chronotype. It is known that as people age their chronotype becomes progressively earlier. There was no significant difference between groups with regards to their chronotypes.

3.2. Vignettes from Study Participants

a.

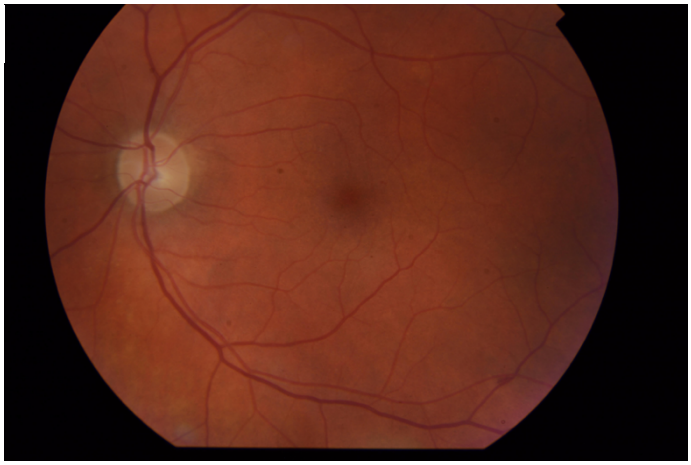

b.

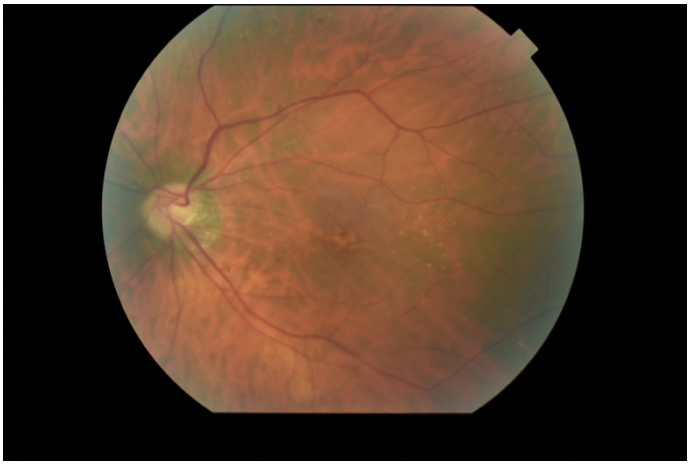

c.

d.

Figure 3.2.1. Fundal photographs taken from **a.** a Category 1 participant, **b.** a Category 2 participant, **c.** a Category 3 participant and **d.** a Category 6 participant.

a

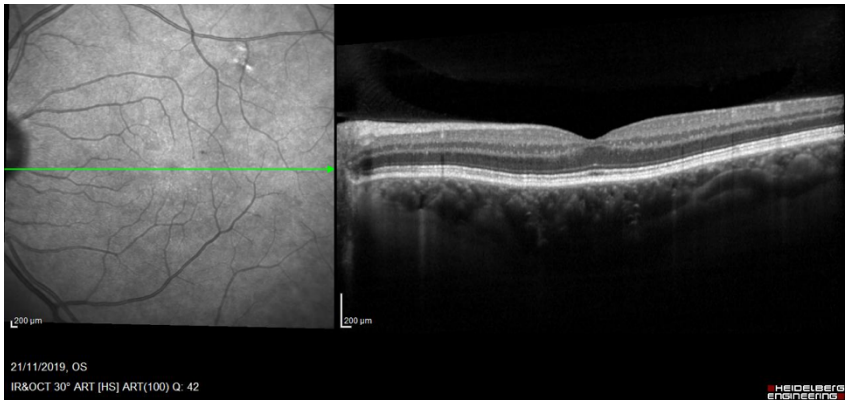

b.

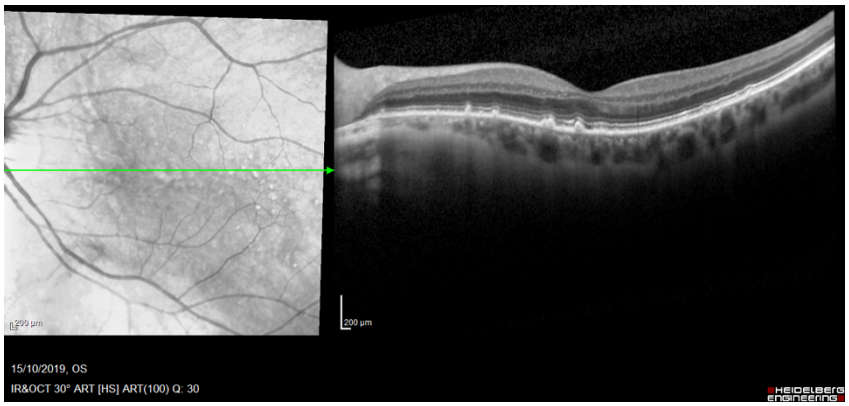

c.

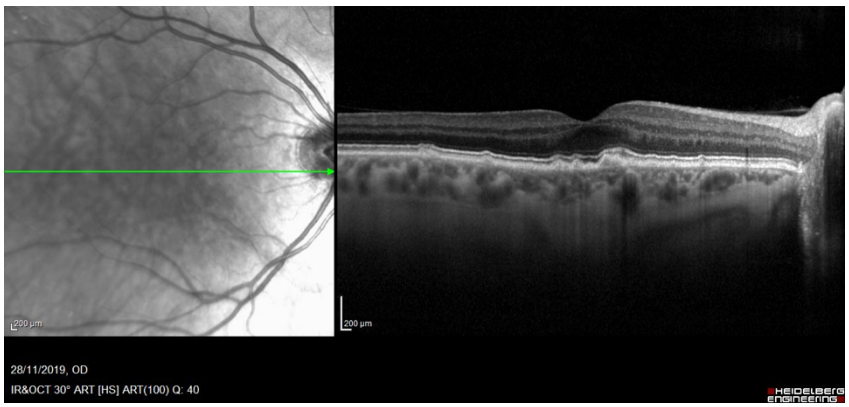

d.

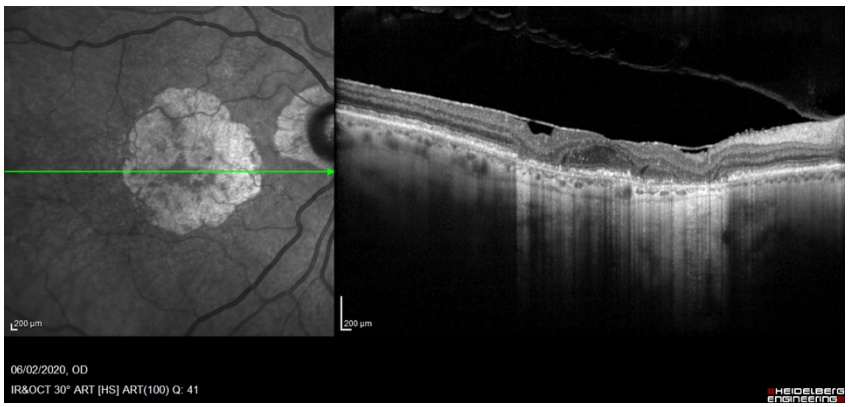

Figure 3.2.2. Optical coherence tomography (OCT) and autofluorescence images from taken from **a.** a Category 1 participant, **b.** a Category 2 participant, **c.** a Category 3 participant and **d.** a Category 6 participant.

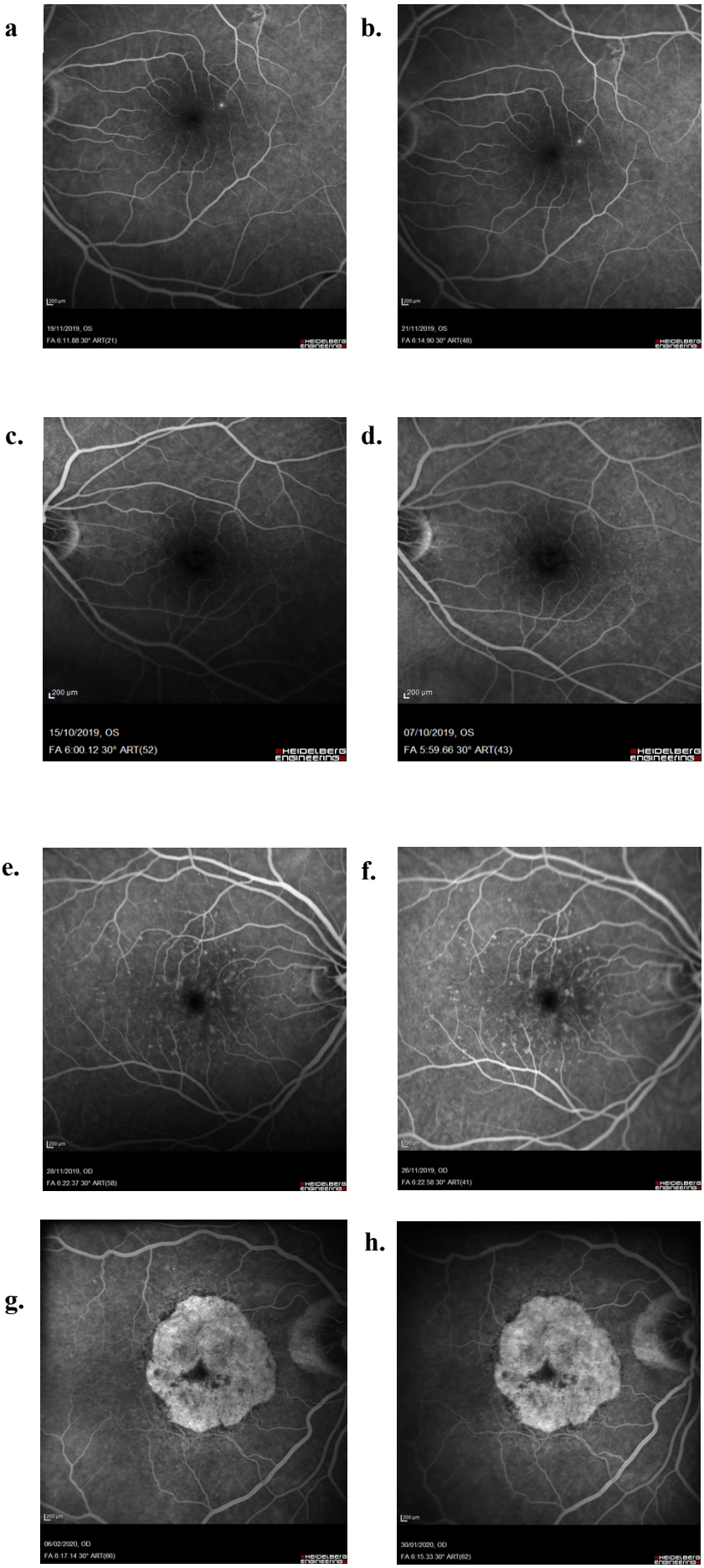

Figure 3.2.3. Fundus fluorescein angiography (FFA) images taken 6 minutes following the administration of sodium fluorescein in: **a.** & **b.** the same Category 1 participant at the AM and PM timepoints respectively; **c.** & **d.** the same Category 2 participant at the AM and PM timepoints respectively; **e.** & **f.** the same Category 3 participant at the AM and PM timepoints respectively; **g.** & **h.** the same Category 6 participant at the AM and PM timepoints respectively.

Figure 3.2.1. demonstrates a colour fundal photograph from a selected participant from each category. There are no drusen present or pigment abnormalities in the category 1 participant, the category 2 participant has >10 small drusen (<63µm), the category 3 participant has >1 drusen >125µm and the category 6 participant has a well-defined area of RPE atrophy with visibility of the underlying choroidal vessels. Figure 3.2.2 demonstrates autofluorescence and OCT images from the same participant as seen in Figure 3.2.1. Notably in the category 2 and 3 participants there are both classical drusen and reticular pseudodrusen present. It is important to identify those participants with reticular pseudodrusen as their presence are associated with a greater risk of progression to late stages of AMD. The category 6 participant has loss of normal foveal contour with RPE atrophy with increased reflectivity of the choroidal layer. Figure 3.2.3. are FFA images at 6 minutes taken at both the AM and PM visits. As these are just snapshots of the FFA images it is difficult to make any assumptions regarding differences in light intensity.

3.3. Automated FFA Analysis

3.3.1. Non-Human Primate Analysis

The FFA results from the manual analysis of the non-human primate cohort (n=6 monkeys, n=12 eyes) using ImageJ have been described in Hudson *et al.,* 2019. In this section the results from the automated analysis of these same images will be discussed and compared to the results of the manual analysis. Of note the NHP subjects were anaesthetised prior to the FFA being performed and for this reason the images contain minimal artefact secondary to eye movement. Figure 3.3.1.1 demonstrates the integrated grey level (IGL) plotted against time for a NHP subject with each graph representing a region of interest. For each graph there is an initial peak in IGL within the first minute following fluorescein administration representing an influx of fluorescein with a subsequent drop and a plateau in IGL level representing fluorescein clearance. In this particular subject, the PM IGL level is greater than the AM level at all regions of interest however it is important to look at the IGL across all subjects in further graphs. Figure 3.3.1.2. represents the probability plots for the NHP data analysis and demonstrates that the data follows a non-parametric distribution so will be analysed using the Wilcoxin rank sum test. Figure 3.3.1.3. represents the cumulative IGL per region of interest and the cumulative IGL percentage difference in all the NHP subjects. The cumulative IGL per region of interest takes the sum IGL data at each time point for each eye. Of note there is no significant change observed here and the error margin is large likely because this incorporates all NHP results combined instead of comparing the AM to PM for one individual subject. For this reason, it is more appropriate to assess the cumulative IGL percentage difference which

measures the sum light intensity in all AM time points vs all PM timepoints for each individual subject. The red is the median and bars are centered around 0 (meaning no difference between AM and PM) and although there is no statistically significant change in AM vs PM, we can see that the results are trending towards an increase in IGL in PM with the highest change in the fovea. As we have observed in Figure 3.3.1.1. however, the IGL varies substantially based on the time following fluorescein administration therefore it is important not only to measure the percentage difference over a specific phase in addition to the percentage difference across all timepoints. This can be seen in Figure 3.3.1.4. where the early phase represents all images captured from fluorescein administration up to two minutes and the mid phase represents images captured from two to six minutes. There is no late phase in this demographic as imaging stopped at six minutes. In the early phase there is a statically significant percentage increase in IGL in the PM session in the fovea only whereas in the mid phase there is a statically significant increase in IGL in the fovea and perifovea. This also corresponds well with the manual FFA analysis as reported by Hudson *et al*., 2019 where the most significant change in intensity in AM vs PM was noted at the six-minute timepoint. Figure 3.3.1.5. represents signal decay in AM and PM at the two- and six-minute mark i.e., the difference between the initial peak and the plateau where the peak is 100% as represented by the line at the top of the graph. There is a statically significant increase in signal decay in the fovea at both timepoints for the AM vs the PM representing a greater remaining IGL signal in the PM vs the AM. Similarly, Table 3.3.1. also measures the rate of signal change however this calculates a slope of the line that best fits the graph of IGL vs time as demonstrated in Figure 3.3.1.6. and uses this to compare AM and PM results. Of note there is no difference noted in the early phase and this is likely as a result of the sharp IGL peak from fluorescein influx. However, in the mid phase in all regions except the fovea the AM slope is steeper representing greater fluorescein clearance.

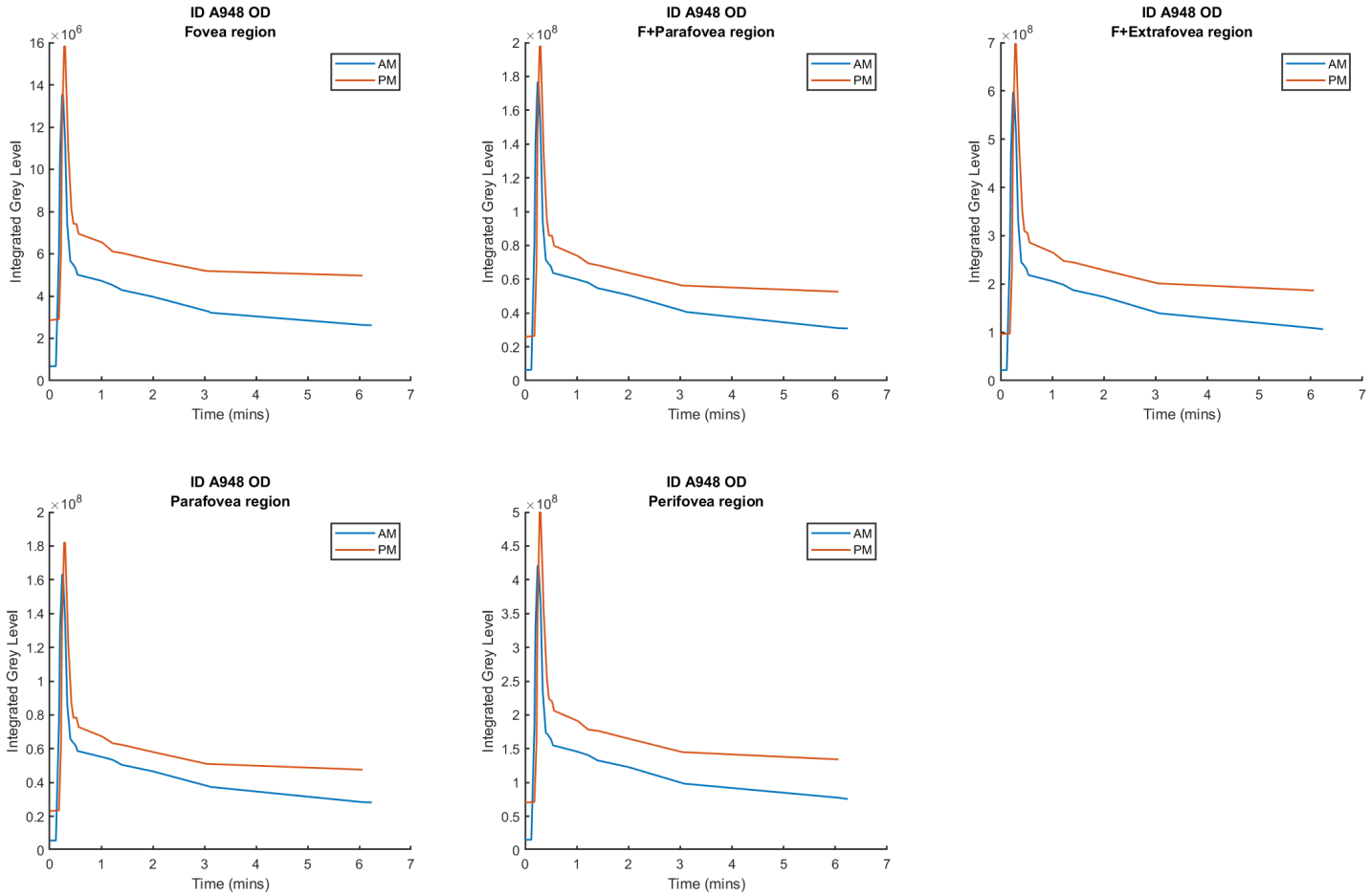

Figure 3.3.1.1. Integrated grey level (interpreted as the sum light intensity) vs time in AM (blue) and PM (red) for each region of the ETDRS grid for one NHP subject (**Figure 2.5.3.2.).**

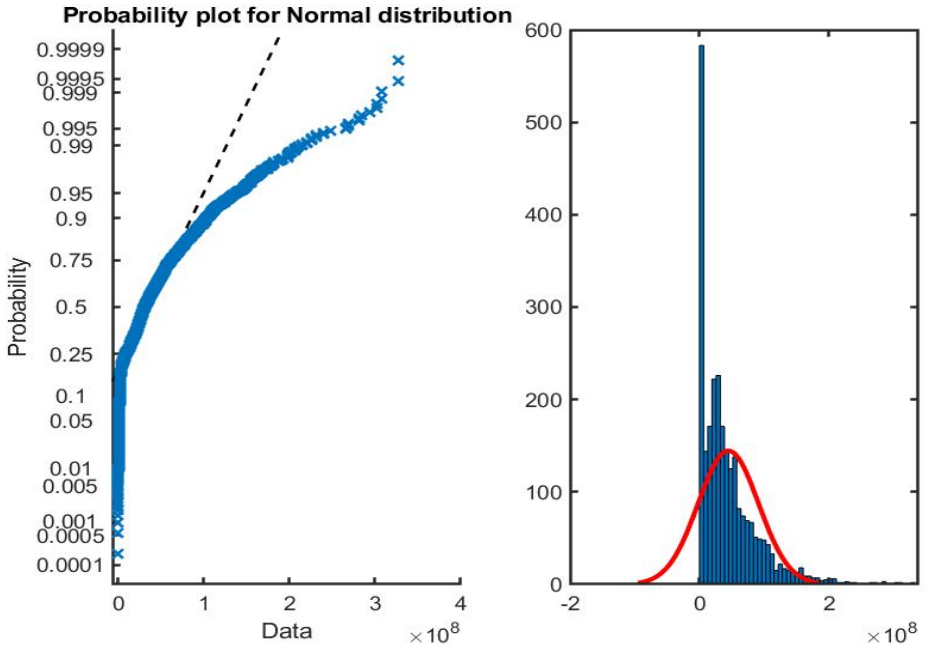

Figure 3.3.1.2. Probability plot for normal distribution for the NHP cohort.

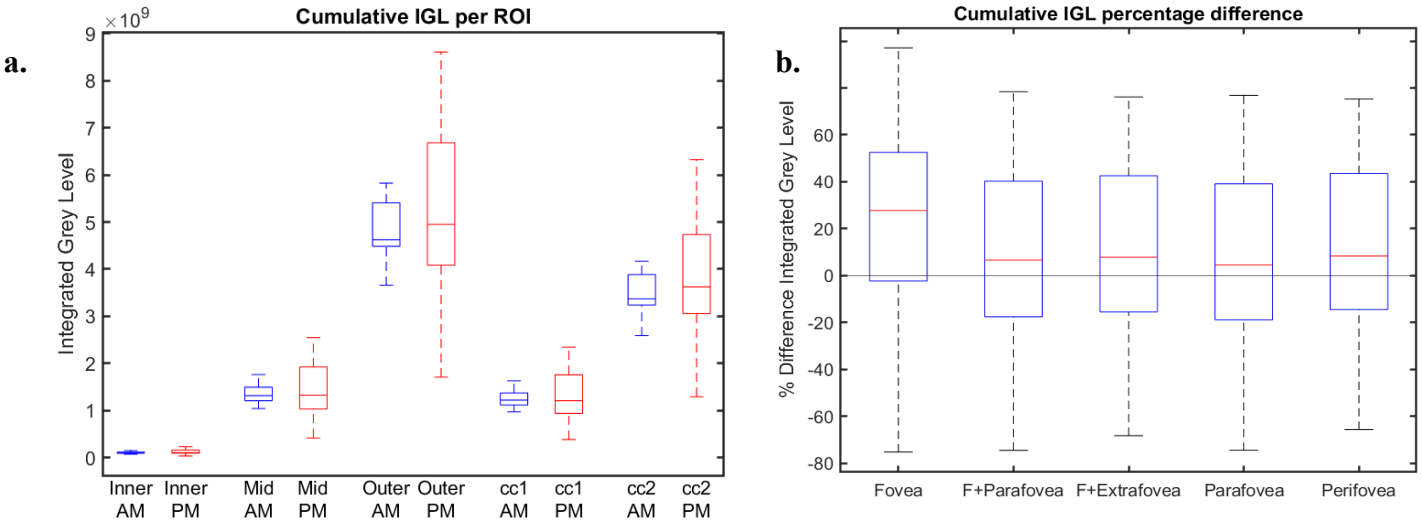

Figure 3.3.1.3. Graph **a.** cumulative integrated grey levels (IGLs) in AM (blue) and PM (red) per region of interest and **b.** cumulative IGL percentage difference between AM and PM for each region of the ETDRS grid.

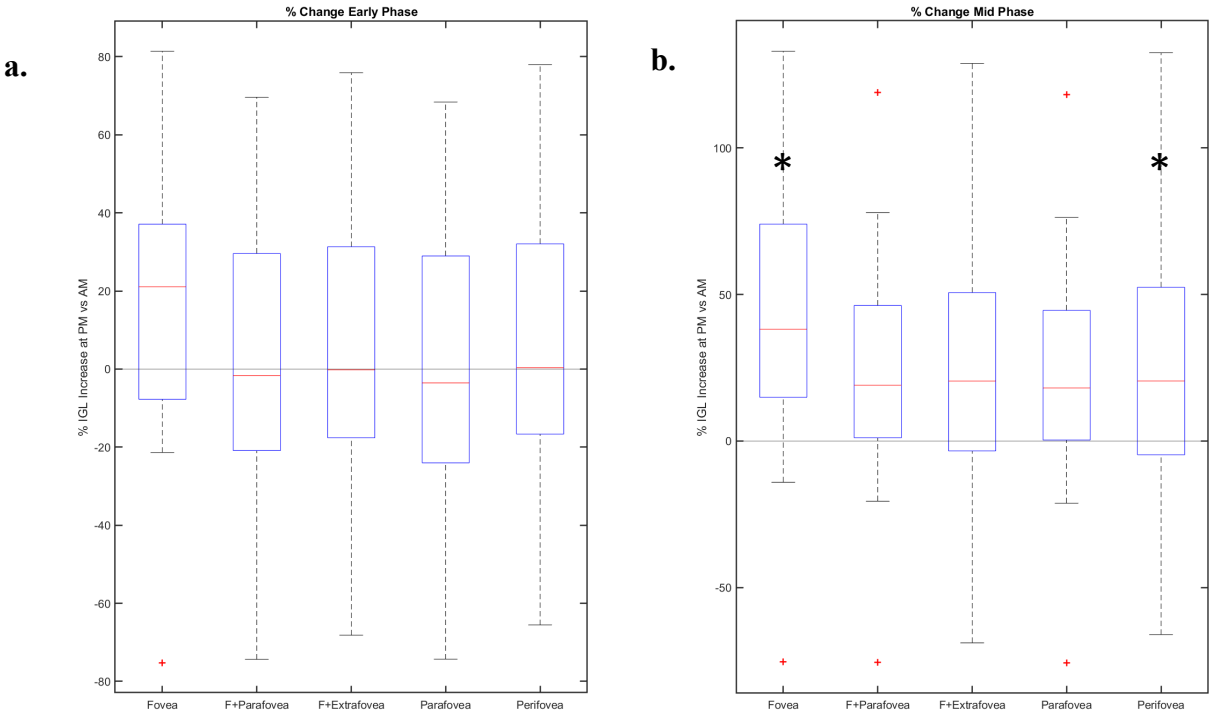

Figure 3.3.1.4. Percentage change in IGL level in PM vs AM in **a.** the early phase and **b.** the mid phase.

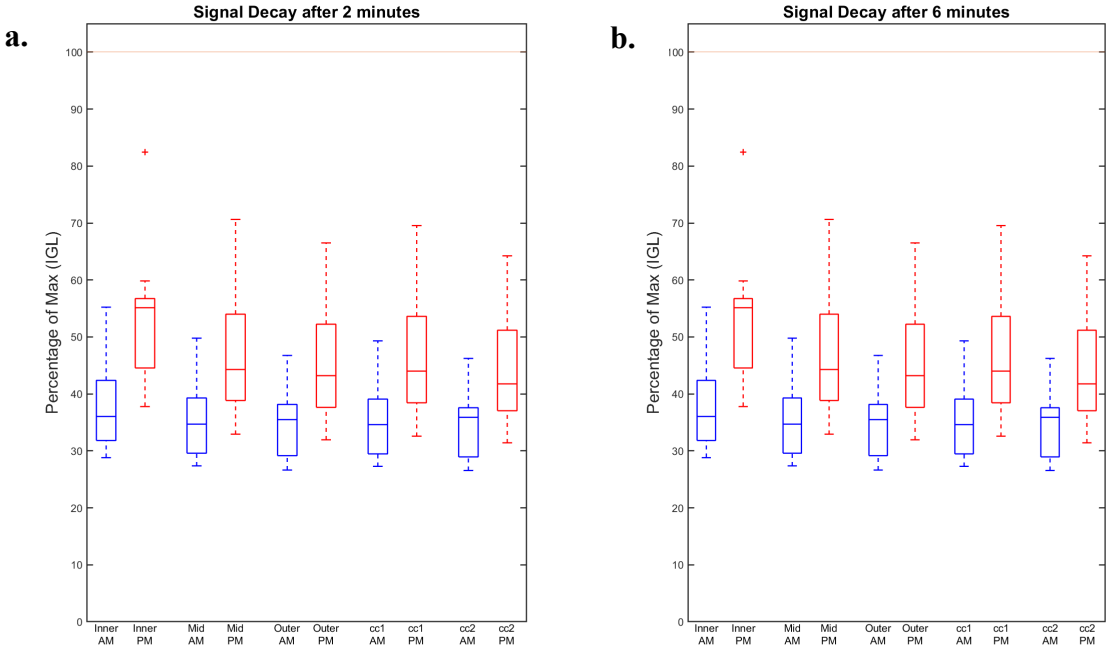

Figure 3.3.1.5. Signal decay of all subjects comparing AM (blue) to PM (red) at two chosen timepoints **a.** 2 minutes and **b.** 6 minutes. The line at 100 represents the maximum signal achieved.

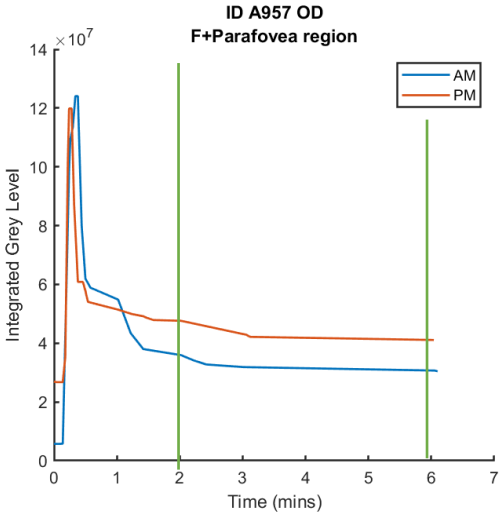

Significant change in median slope at AM vs PM?		
Region	**Early Phase**	**Mid Phase**
Foveal	No	No
Foveal + parafoveal	No	Yes
Foveal + extrafoveal	No	Yes
Parafoveal	No	Yes
Perifoveal	No	Yes

Figure 3.3.1.6. and **Table 3.3.1.** Rate of signal change in AM vs PM for one NHP at the fovea and parafoveal region in the graph and the cumulative change across all subjects in the table.

3.3.2. Healthy Young Participant Analysis

As in the NHP cohort, the results of the manual FFA analysis using ImageJ for the healthy young participant group (n=15) have been described in Hudson *et al.,* 2019. Here we will discuss the automated analysis of this cohort with the addition of more participants to bring the participant number to n=28. Images were captured every 15 seconds for 10 minutes. Unlike the NHP the participants were not anaesthetised prior to FFA imaging, for this reason there is more artefact noted due to participant head or eye movement in between image capture. This leads to a greater variability between images for example participant movement leads to some images being darker than predicted with respect to other images in the sequence. In order to minimise variability, we have selected four of the best quality images at each phase for analysis. One of the major notable differences between the NHP and healthy young participant cohorts is that the human FFA images do not demonstrate the initial IGL peak which corresponds to the initial fluorescein influx (as seen in Figure 3.3.2.1). This peak is likely also present in the human participants but may be missed as the participants are not anaesthetised and the conditions are not as controlled as in the NHP cohort. For this reason we are unable to calculate the signal decay in the human participants. As with the NHP cohort, the probability plot for data analysis demonstrates that the data follows a non-parametric distribution. For the cumulative IGL per ROI (Figure 3.3.2.3. a.) there is greater variability noted as demonstrated by larger error bars, this is likely secondary to greater artefact in imaging. Looking at the cumulative IGL percentage difference (Figure 3.3.2.3. b.) the percentage increase in PM cumulative IGLs are significantly increased in both the foveal and parafoveal regions. In comparison to the NHP cohort, in the phase comparison we have data from the early and mid-phase along with the late phase (six- to ten-minutes) and have also analysed the phase comparison at six minutes as this was the timepoint where the major difference between AM and PM light intensity manifested. Notably there was a statistically significant percentage change in PM vs AM in all regions in the mid-phase and six-minute time point and in the fovea in the late phase. This is in keeping with the manual FFA analysis in this same cohort. There is substantial variability in the rate of signal change secondary to artefact and the only region with a significant change in the median slope at AM vs PM is in the fovea in the mid-phase (Table 3.3.2.).

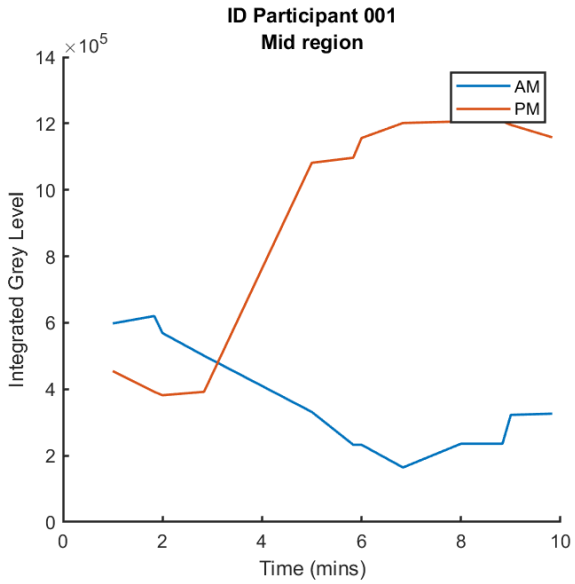

Figure 3.3.2.1. IGL vs time for a participant in the healthy young control cohort in AM (blue) and PM (red)

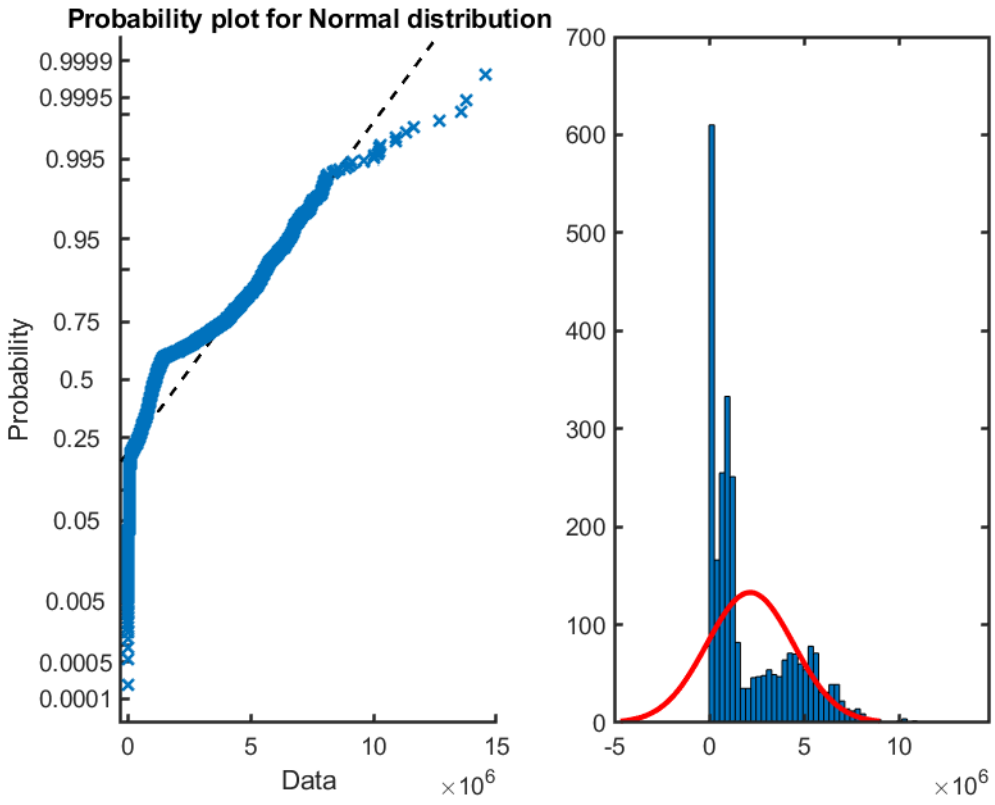

Figure 3.3.2.2. Probability plot for normal distribution for the healthy human control cohort.

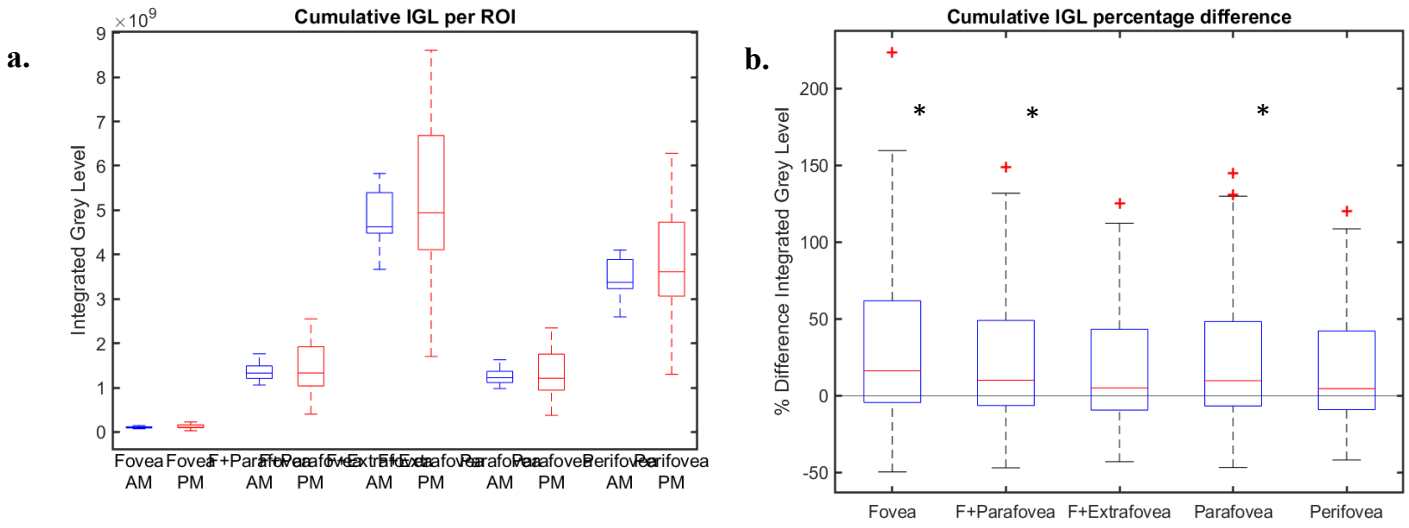

Figure 3.3.2.3. Graph **a.** cumulative integrated grey levels (IGLs) in AM (blue) and PM (red) per region of interest and **b.** cumulative IGL percentage difference between AM (blue) and PM (red) for each region of the ETDRS grid.

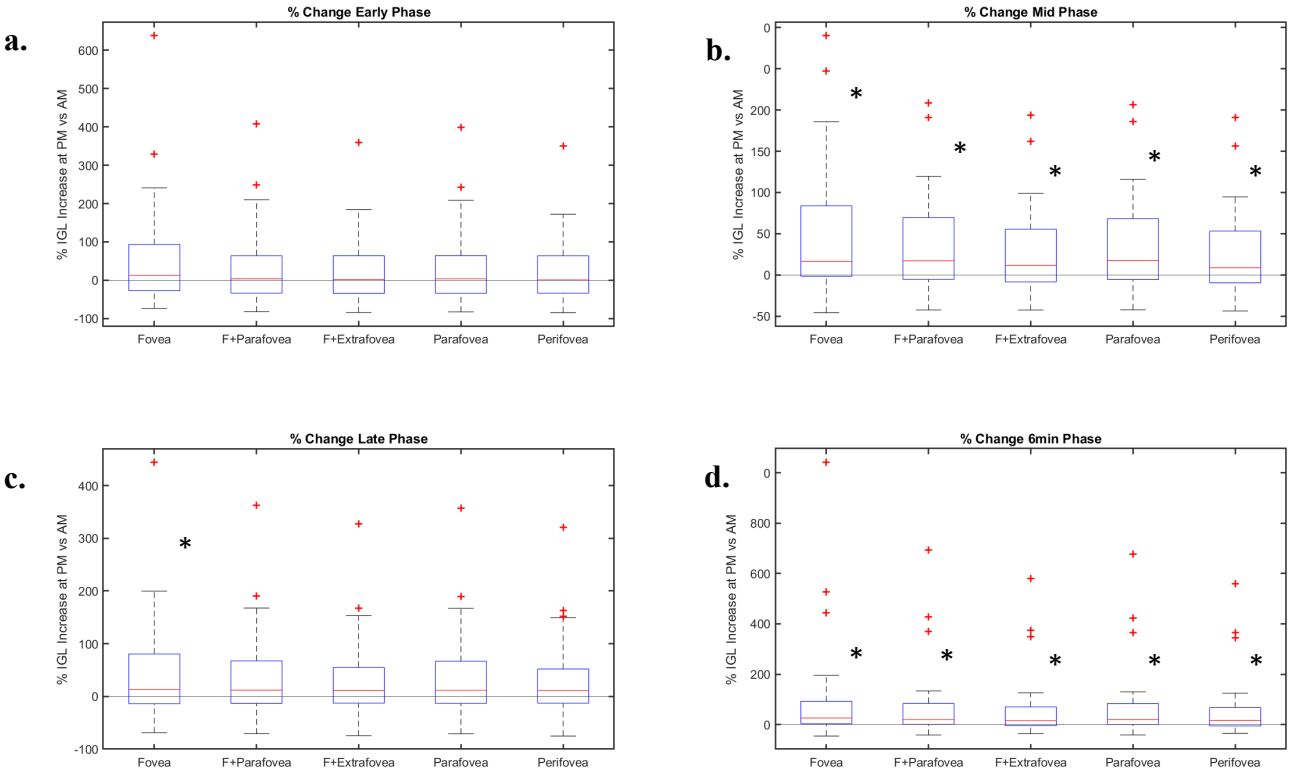

Figure **3.3.2.4.** Percentage change in IGL level in PM vs AM in **a.** the early phase, **b.** the mid phase, **c.** the late phase and **d.** at the 6-minute phase.

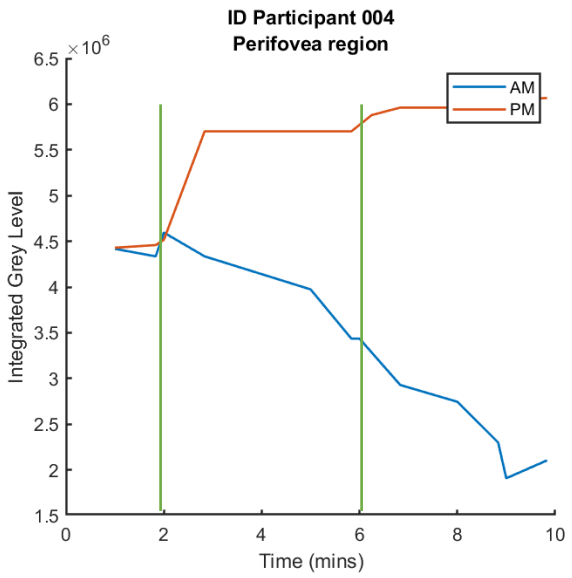

Significant change in median slope at AM vs PM?			
Region	**Early Phase**	**Mid Phase**	**Late Phase**
Foveal	**No**	**Yes**	**No**
Foveal + parafoveal	**No**	**No**	**No**
Foveal + extrafoveal	**No**	**No**	**No**
Parafoveal	**No**	**No**	**No**
Perifoveal	**No**	**No**	**No**

Figure 3.3.2.5. and **Table 3.3.2.** Rate of signal change in AM vs PM for one individual participant at the perifoveal region in the graph and the cumulative change across all participants in the table.

3.3.3. AMD Participant Analysis

The results discussed here represent new data collected between July 2019 and February 2020 as discussed in the methods section. Due to limited numbers (n=16) all AMD participants from category 2 to category 6 were combined into one AMD participant group. As the study numbers increase, we will be in a position to separate these groups for analysis. All images taken for each participant were analysed unlike the healthy young control group where the best four images at each phase were selected. FFA imaging in this older demographic proved to be more difficult than in the young healthy control group as participants often had difficulties in remaining in the same position for the duration of imaging. Subsequently, we modified the process by which images were captured aiming to obtain a series of good quality photographs at each minute mark. Despite this adaptation however there were still substantial artefacts noted in the images. This is reflected in large error bars and marked peaks and troughs of IGL when compared to time which are not in keeping with the parameters set in the NHP cohort (Figure 3.3.3.1.). As in the NHP and young healthy control cohorts the data was non-parametrically distributed (Figure 3.3.3.2.). There was no difference in cumulative IGL per

ROI or in cumulative IGL percentage difference (Figure 3.3.3.3.). Interestingly, although there is no statistically significant change in PM signal compared to AM signal at each phase or six-minute timepoint in the mid-phase there appears to be a downward trend (i.e., a decrease in PM signal vs AM signal) which could potentially indicate a change to the normal homeostasis in the AMD group. There is no significant change in the slope of the signal between AM and PM at each phase.

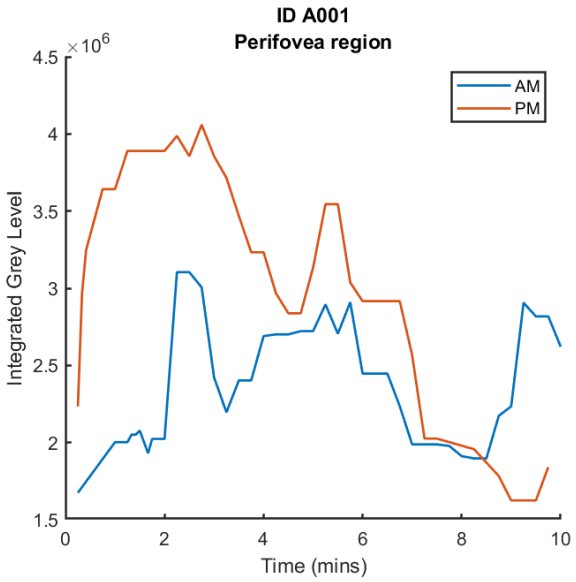

Figure 3.3.3.1. IGL vs time for a participant in the AMD participant group.

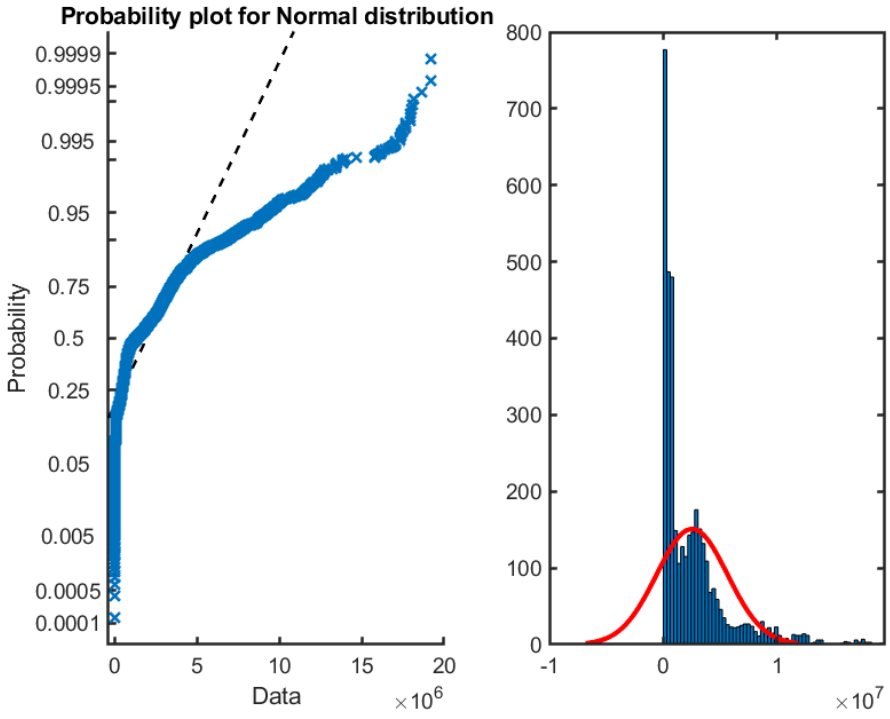

Figure 3.3.3.2. Probability plot for normal distribution for the AMD participant group.

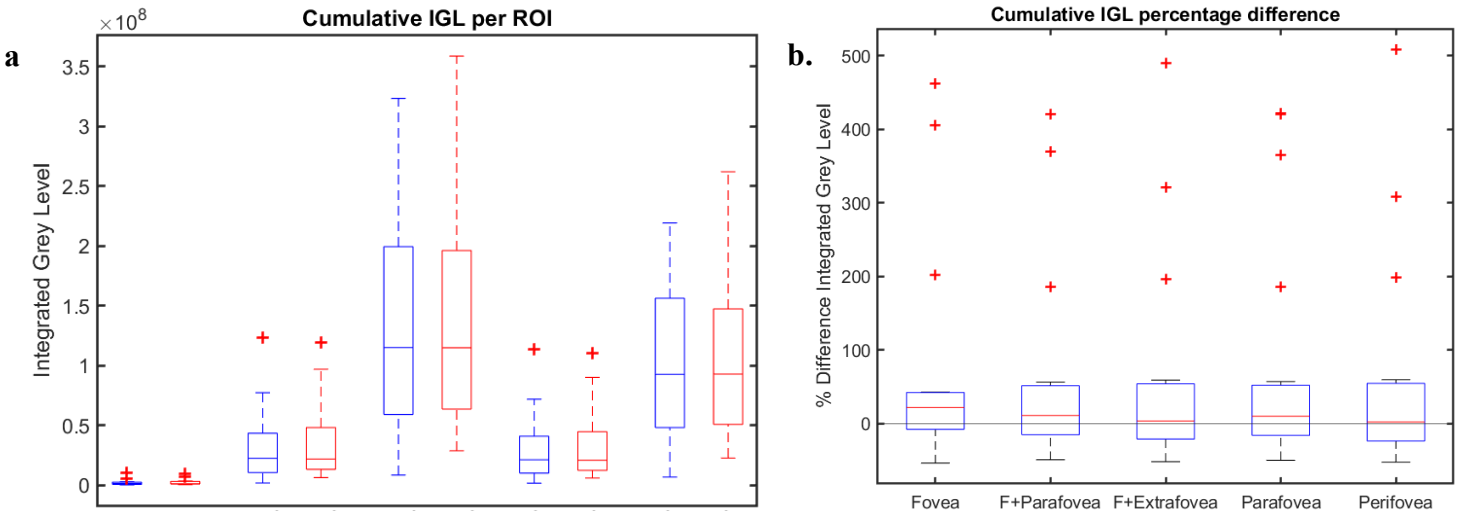

Figure 3.3.3.3. Graph **a.** representing cumulative integrated grey levels (IGLs) in AM (blue) and PM (red) per region of interest and **b.** representing cumulative IGL percentage difference. between AM (blue) and PM (red) for each region of the ETDRS grid.

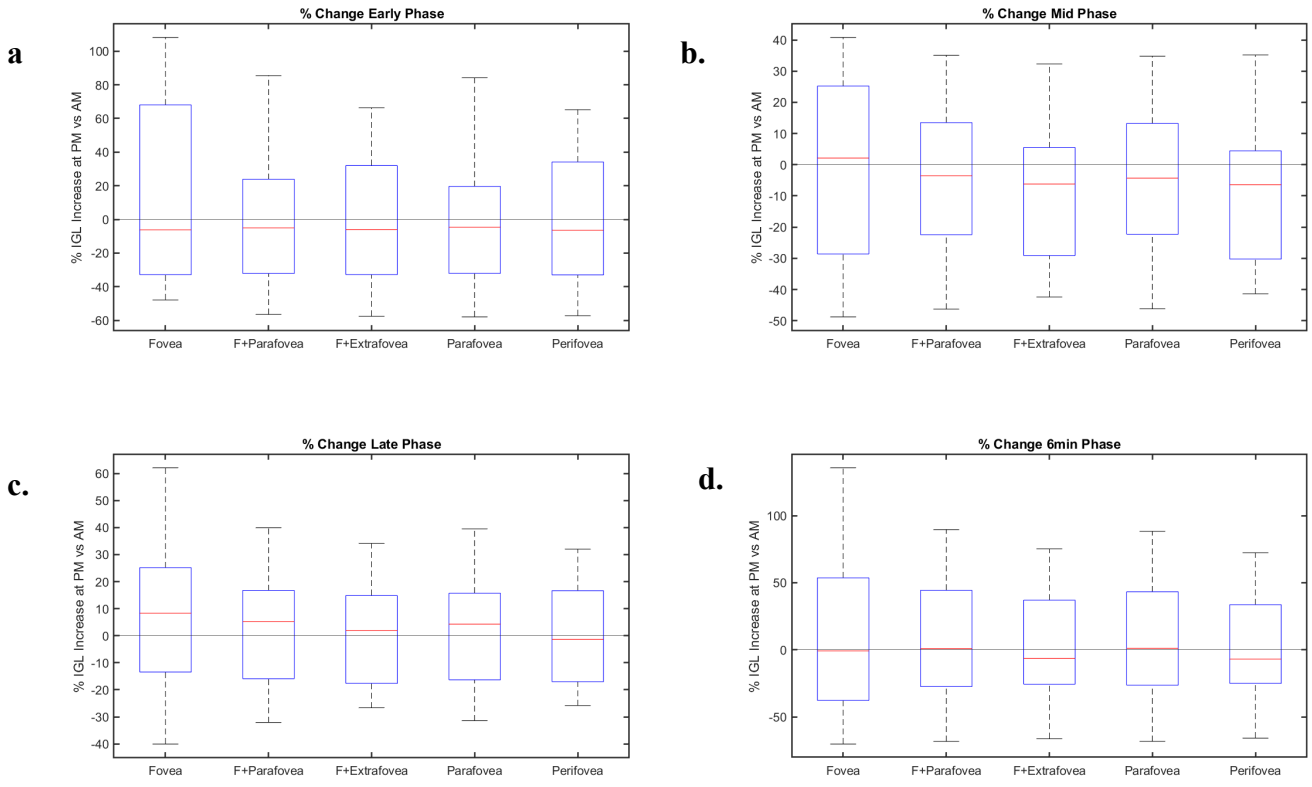

Figure 3.3.3.4. Percentage change in IGL level in PM vs AM in **a.** the early phase, **b.** the mid phase, **c.** the late phase and **d.** at the 6-minute phase.

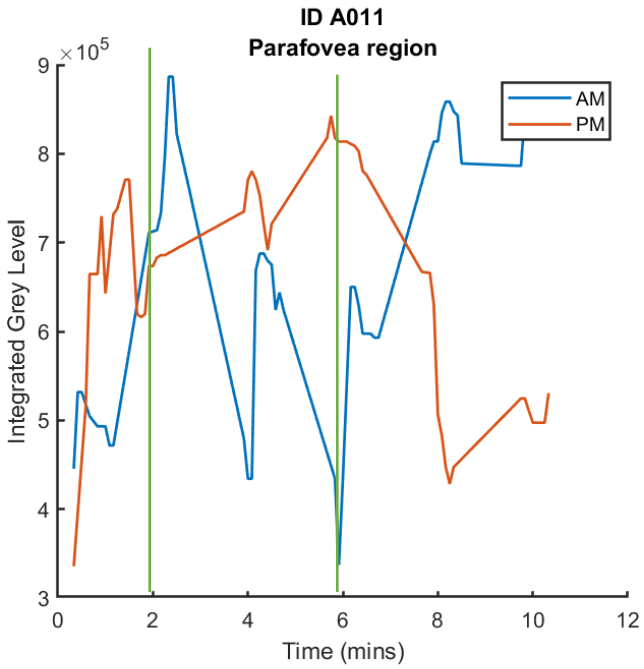

Significant change in median slope at AM vs PM?			
Region	**Early Phase**	**Mid Phase**	**Late Phase**
Foveal	**No**	**No**	**No**
Foveal + parafoveal	**No**	**No**	**No**
Foveal + extrafoveal	**No**	**No**	**No**
Parafoveal	**No**	**No**	**No**
Perifoveal	**No**	**No**	**No**

Figure 3.3.3.5. and **Table 3.3.3.** Representing rate of signal change in AM vs PM for one individual participant at the parafoveal region in the graph and the cumulative change across all participants in the table.

3.3.4. Healthy Age-Matched Control Analysis

The results discussed here represent new data collected between July 2019 and February 2020 as discussed in the methods section. Of note there are limited numbers (n=9) in this participant group, we aim to expand these numbers as the study continues. Again, as in the AMD participant group all the images were analysed, and the quality was similar to the AMD participant group (Figure 3.3.4.1.) As with the other groups data was non-parametrically distributed as demonstrated in Figure 3.3.4.2. There is no statistically significant difference in cumulative IGL per ROI in AM vs PM or in cumulative IGL percentage difference in AM vs PM however it should be noted that the sample number is likely too low to establish statistical significance and there is a trending increase in PM however it is still 0 (Figure 3.3.4.3.). Similarly, in the phase comparison is no statistically significant change in any of the phases however the mid phase is trending towards significance with a percentage increase in PM. In the mid-phase in all regions except the fovea there is a significant change in the median slope in AM vs PM.

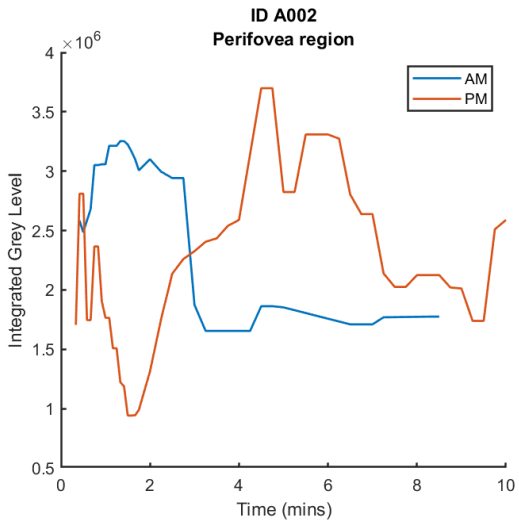

Figure 3.3.4.1. IGL vs time for a participant in the age-matched control group.

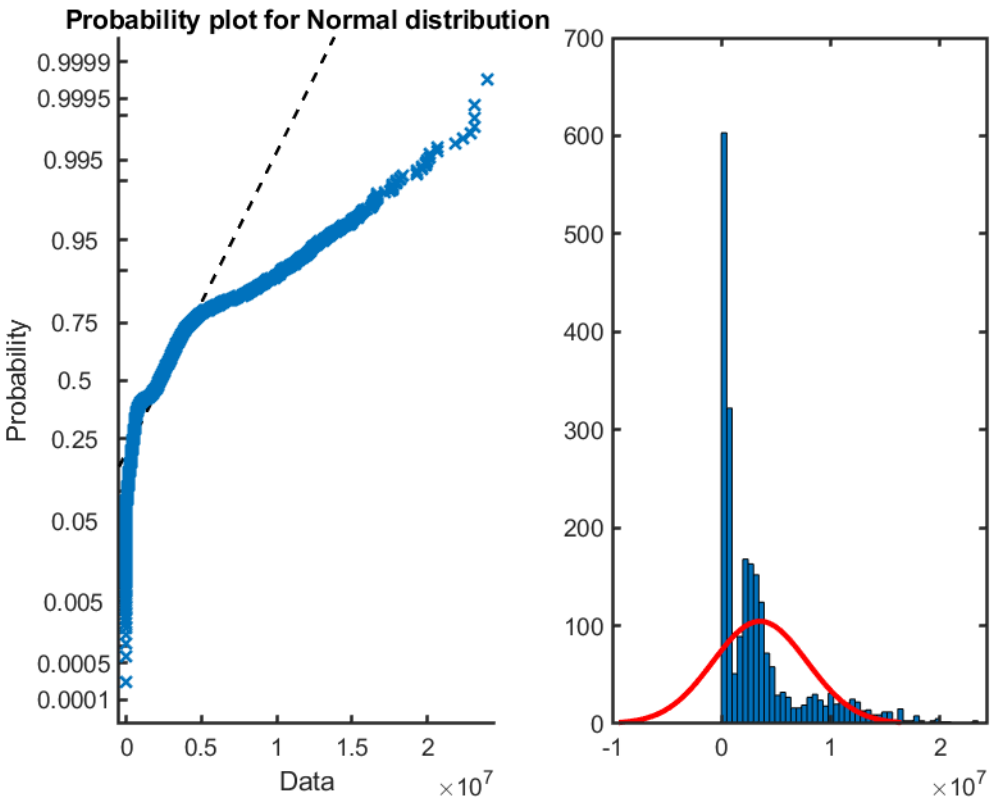

Figure 3.3.4.2. Probability plot for normal distribution for the AMD participant group.

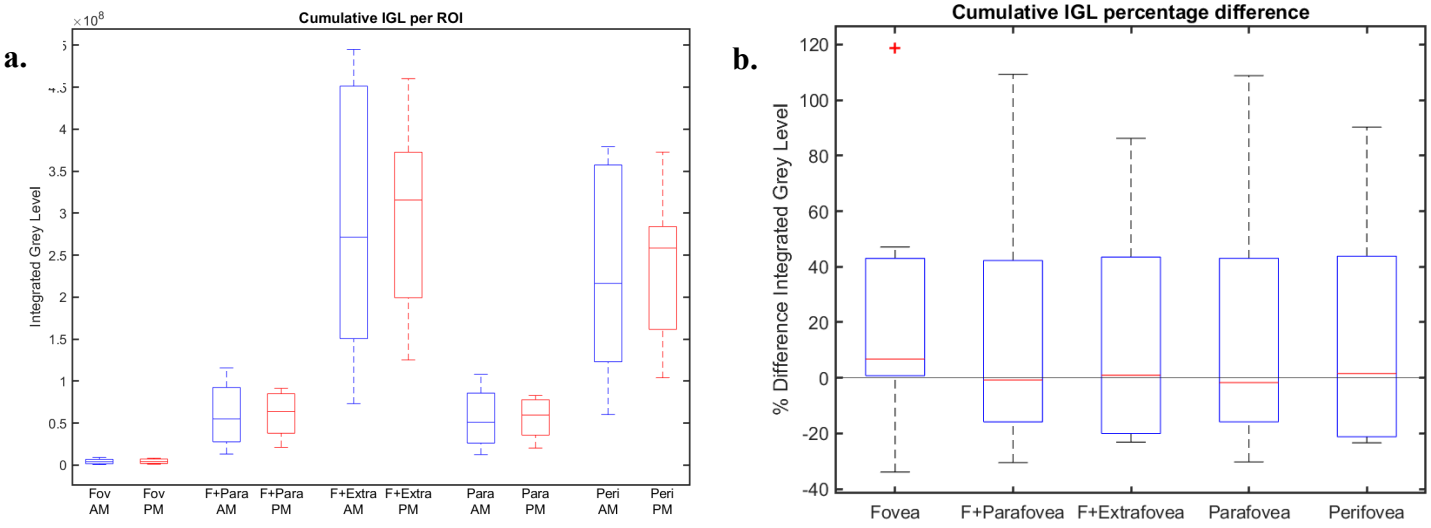

Figure 3.3.4.3. Graph **a.** cumulative integrated grey levels (IGLs) in AM (blue) and PM (red) per region of interest and **b.** cumulative IGL percentage difference between AM (blue) and PM (red) for each region of the ETDRS grid.

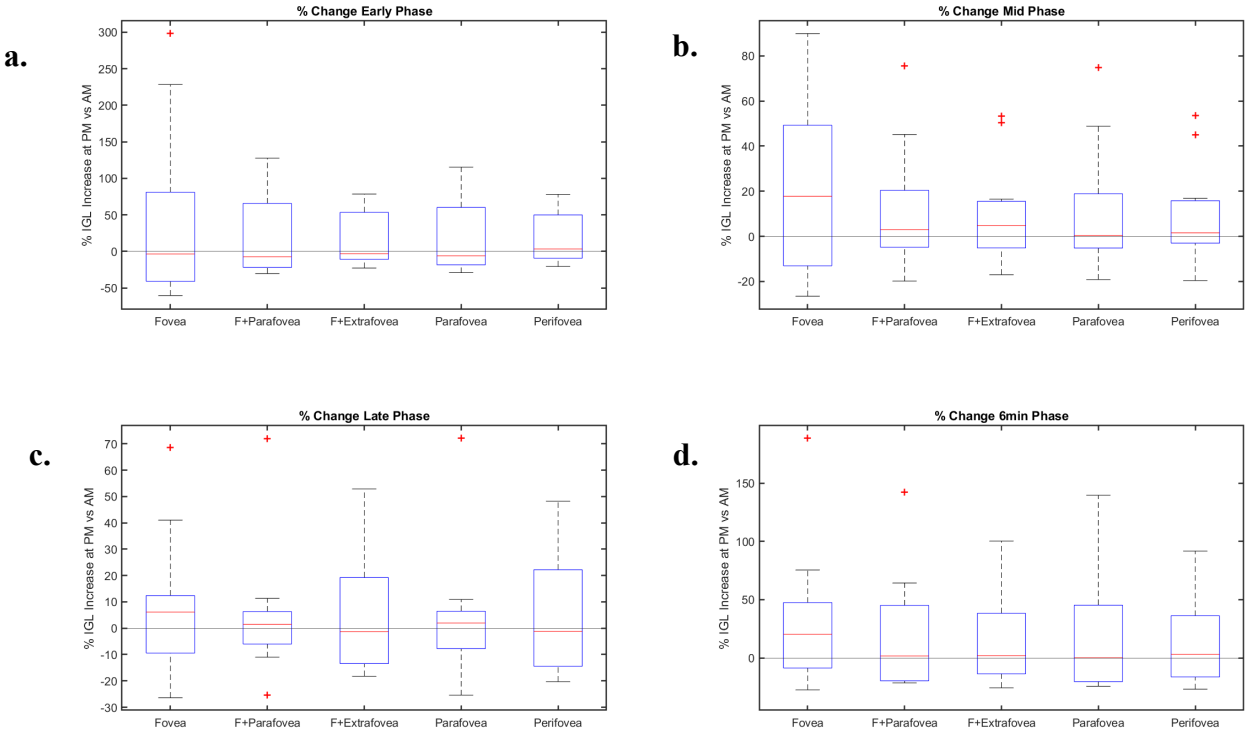

Figure 3.3.4.4. Percentage change in IGL level in PM vs AM in **a.** the early phase, **b.** the mid phase, **c.** the late phase and **d.** at the 6-minute phase.

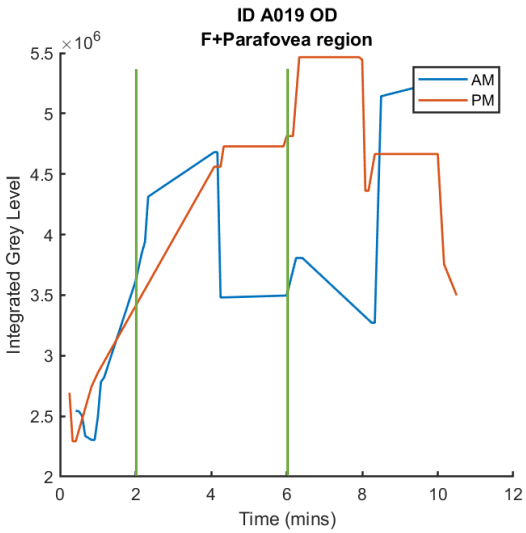

Significant change in median slope at AM vs PM?			
Region	**Early Phase**	**Mid Phase**	**Late Phase**
Foveal	No	No	No
Foveal + parafoveal	No	Yes	No
Foveal + extrafoveal	No	Yes	No
Parafoveal	No	Yes	No
Perifoveal	No	Yes	No

Figure 3.3.4.5. and **Table 3.3.4.** Representing rate of signal change in AM vs PM for one individual participant at the foveal and parafoveal region in the graph and the cumulative change across all participants in the table.

3.4. OCT Analysis for the AMD and Age-Matched Control Participants:

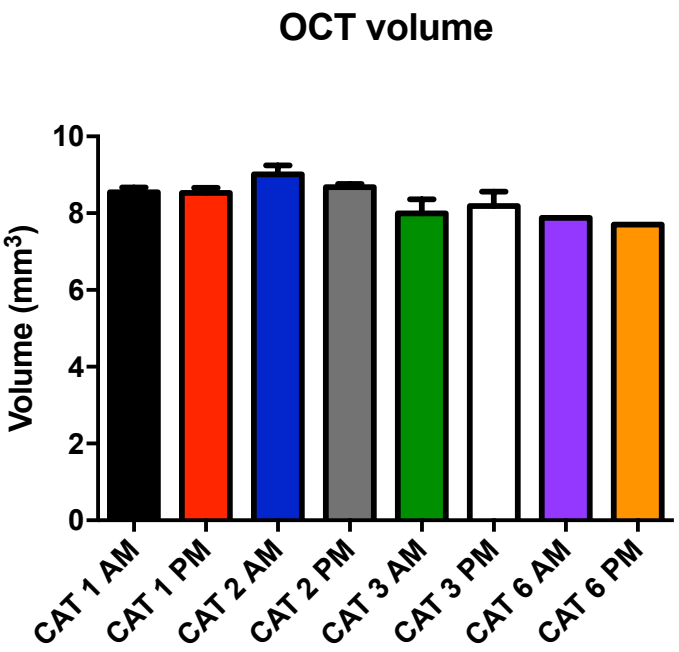

Figure 3.4.1. Total OCT volume for each category of participant at AM and PM.

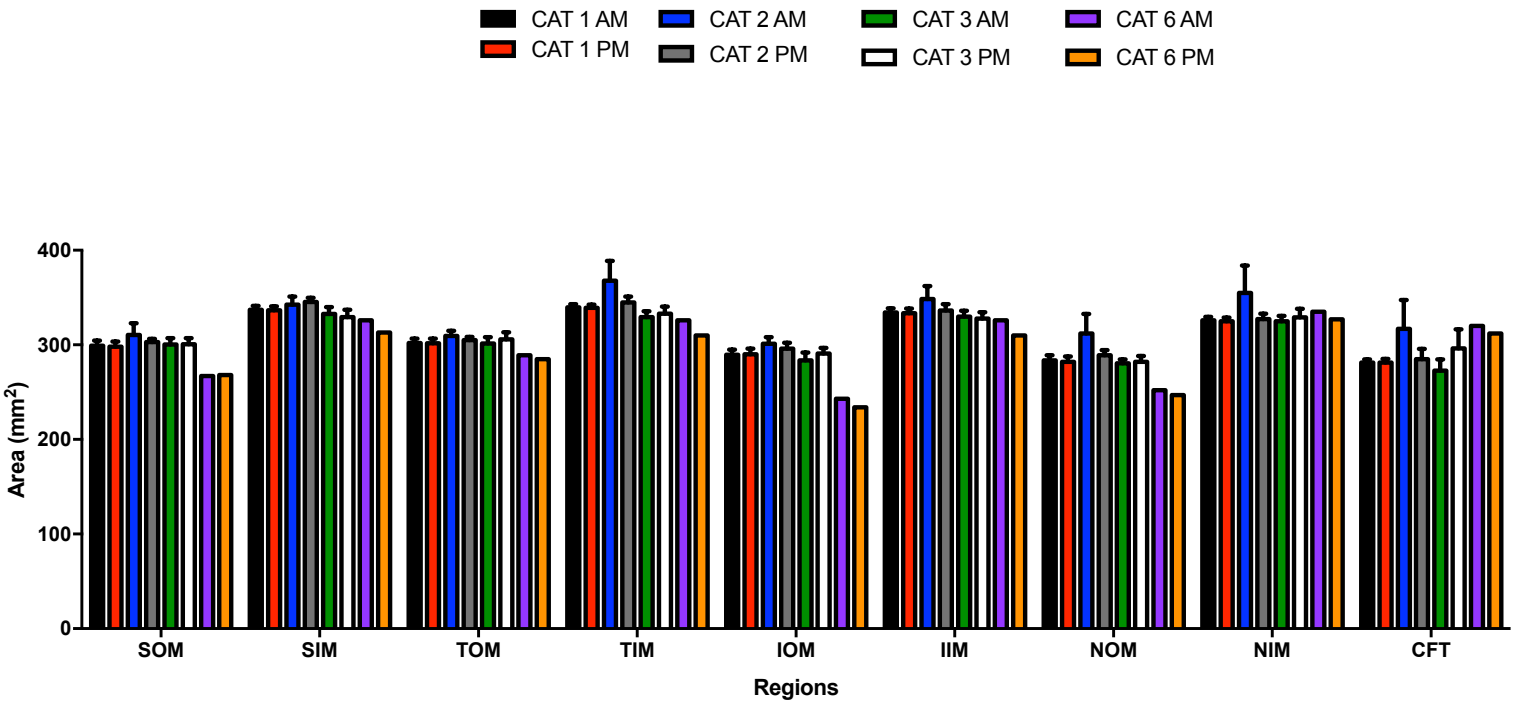

Figure 3.4.2. Total OCT area for each participant category per ETDRS region; superior outer macula (SOM), superior inner macula (SIM), temporal outer macula (TOM), temporal inner macula (TIM), inferior outer macula (IOM), inferior inner macula (IIM), nasal outer macula (NOM), nasal inner macula (NIM) and central foveal thickness.

OCT analysis confirms that there is no significant change between AM and PM in total OCT volume in any participant cohort. Furthermore, is there no significant change in OCT area in any ETDRS region between AM and PM for all participant groups. This is in keeping with the results in the healthy young control analysis. As discussed in Chapter 1, although studies have demonstrated diurnal variation in retinal thickness in DMO and CRVO there have not been studies specifically investigating at diurnal variations in retinal thickness in AMD. Furthermore, results have been mixed with regards to diurnal variation of retinal thickness in healthy individuals. Going forward it would be beneficial to analyse the thickness of individual retinal layers, especially as Read *et al.,* 2012 have demonstrated that a significant diurnal variation occurs in the thickness of the foveal outer layers, with the most prominent changes occurring in the photoreceptor layers at the foveal centre. This may prove to be of particular interest as the pathology in AMD manifests in these retinal layers.

Table 3.4 compares the number and stage of reticular pseudodrusen in each participant category. As we have discussed previously the presence of reticular pseudodrusen confer a risk of progression to both forms of advanced AMD independent of classical drusen. Two participants in category 2 and all participants in category 3 were found to have at least one reticular pseudodrusen present on OCT. This is important to note as these individuals are at a higher risk of AMD progression.

Grading Category	Stage of Reticular Pseudodrusen			
	Stage 1	Stage 2	Stage 3	No reticular pseudodrusen
Category 1 (n=9)	0	0	0	9
Category 2 (n=6)	1	1	0	4
Category 3 (n=11)	1	8	2	0
Category 6 (n=1)	0	0	1	0

Table 3.4. Number and grade of reticular pseudodrusen present in each participant grading category. The staging system used for reticular pseudodrusen is described in Zweifel *et al.,* 2010. Stage 1 is defined by a diffuse deposit of granular hyperreflective material between the RPE and ellipsoid layer. Stage 2 represents the progression of material accumulation between

the RPE and ellipsoid forming mounds which distort the contour of the ellipsoid layer. Stage 3 represents conical shaped reticular pseudodrusen which punch through the ellipsoid layer.

CHAPTER 4: Discussion

4.1 Implications of Results

The focal point of this investigation was to continue the clinical arm of the research by Hudson *et al.,* 2019 by making a full assessment of circadian iBRB regulation in patients with defined degrees of dry AMD and age-matched controls. As this was the first year of a study which is predicted to continue over a number of years the emphasis was on establishing study methodology including recruitment, inclusion and exclusion criteria, grading systems, testing protocols, participant safety and optimal imaging techniques.

It is well documented that AMD is a leading cause of central visual impairment worldwide with a further projected increase in prevalence as a result of exponential aging. The condition represents a significant public health issue not only as it has a substantial impact on patients' quality of life and ability to carry out activities of daily living but also as it carries a significant financial burden to the state. Despite the wealth of research into the condition there are currently no treatments available for GA. Furthermore, the progression from early AMD to late AMD remains unpredictable and the molecular pathology underlying the condition remains unclear. The majority of AMD research to date has focused specifically on the RPE and photoreceptors as this is where the pathology manifests. However, Hudson *et al.,* 2019 have demonstrated an inner-retina derived contribution to RPE pathology which may play an important role in the pathogenesis of AMD. We propose that a circadian entrained cycling of inner retinal vasculature permeability is an integral factor in establishing retinal interstitial kinesis which allows for the daily clearance of material from the neural retina and the replenishment of essential substrates to the photoreceptors. We postulate that a chronic and size-selective disruption of the iBRB will lead to a downstream accumulation of material in the RPE over a prolonged period. In the aging eye with circadian clock dysregulation this retinal interstitial kinesis will be less tightly regulated leading to the accumulation and overload of the RPE with spent metabolites and dietary components with resultant drusen formation and RPE atrophy.

Hudson *et al.,* 2019 demonstrated that the gene *CLDN5* which encodes claudin-5 cycles in a distinct circadian rhythm regulated by *BMAL1* and the circadian clock. Claudin-5 transcript levels varied depending on the time of day of tissue collection, with transcript levels being lower in the evening when compared to the morning in all tissues examined. In addition, persistent suppression of claudin-5 expression in mice exposed to a cholesterol-enriched diet

induced RPE depigmentation and atrophy and persistent targeted suppression of claudin-5 in the macular region of non-human primates also induced aberrant RPE structure. It is essential to note that claudin-5 is not expressed in the RPE which strongly suggests a passive paracellular diffusion of material from the systemic circulation toward to RPE. Hudson *et al.,* 2019 also demonstrated that the iBRB is highly dynamic with the macula in humans and nonhuman primates being more permeable in the evening than the morning. This permeability correlates to a decrease in claudin-5 expression in the evening. FFA imaging performed in healthy, young participants aged between 18 and 30 years old indicated that fluorescein signal was evident and more prolonged in the evening compared to the morning in the same subject. This phenotype was also observed in non-human primates. These clinical findings form the basis for our current research as we have extended this study to participants with AMD and age-match controls.

We propose that the normal homeostatic iBRB cycling will cease in AMD subjects. This should manifest as no difference in IGL between the morning and evening images or a reverse where the IGL is greater in the morning than evening. Age-matched controls were also examined to ensure any differences in permeability were not secondary to age-related core clock component dysregulation. Examining our results for the percentage IGL change per-phase for PM vs AM offers an indication that this may in fact be true. In the mid-phase we have demonstrated a downward trend in the AMD participant group and an upward trend in the age-matched control group along with the healthy young control and NHP groups. Although this is not statistically significant in the AMD or age-matched group it indicates a decrease in IGL in PM vs AM in the AMD participants in contrast to an increase in IGL in PM vs AM in all other participant groups. This would represent a change in the normal homeostatic iBRB cycling. If our hypothesis is correct dysregulated circadian mediated cycling of the iBRB could be an early indicator of AMD initiation or progression and restoring cycling by developing a novel form of gene therapy could prevent the development of GA.

There are some notable limitations to our study including limited participant numbers and issues with image quality and artefact. Although we had intended on recruiting 25 AMD participants and 15 age-matched control participants our actual numbers were 18 and 9 participants respectively. Unfortunately, our recruitment was halted early due to Covid-19 and the potential risks associated with bringing elderly participants into a hospital setting. In order to power the study sufficiently and produce significant results the participant numbers in all categories including GA and wet AMD participants need to be expanded further. Due to the limited numbers, we have grouped all AMD participants together into one category for analysis. As the study continues over the coming years it would be beneficial to analyse each group independently to determine if there is a greater disruption to iBRB homeostasis as the

disease progresses and if the iBRB cycling is still preserved in those with early AMD. Furthermore, it would be interesting to compare iBRB cycling in those with and without reticular pseudodrusen as these are a known risk factor for AMD. With regards to image quality, going forward we will amend our process to ensure we have several good quality images at key timepoints which include initial fluorescein administration then at two minutes, four minutes, six minutes, eight minutes and ten minutes to allow for ease of comparison between groups and to minimise artefact.

Although the results have not been discussed here, we also intend on screening the peripheral blood samples for circadian markers including cortisol and melatonin along with RNA levels of BMAL-1, Per2 and Rev-alpha to elucidate molecular changes in circadian rhythm associated transcripts in each individual. Genotyping will also be performed to determine if there is a link between severity of disease, risk variant and changes in iBRB integrity and vessel permeability. These will be performed in the next year of the study.

Another focus of this research was to devise a programme for automated FFA analysis to ensure result validity, repeatability and time efficiency. This programme was initially used to analyse the NHP subject and young healthy control participants and was compared to the manual analysis using ImageJ as discussed in Hudson *et al.,* 2019. As these results appear to correspond well with the manual analysis the programme was then used to analyse the AMD and age-matched control participants' images. Going forward the automated FFA analysis should replace the manual ImageJ based analysis.

Overall, the focal point of establishing study methodology was met with the recruitment of a total 27 participants and an expansion to n=28 young healthy controls. Although the numbers are still too low to provide statistically significant results our initial analysis suggests there may be a cessation of homeostatic iBRB cycling in the AMD cohort vs the age-matched control, healthy young control and NHP cohorts. This needs to be examined further with an increase in study numbers not only in the age-matched control, early mild and early moderate but also an expansion to include all grade of AMD including GA and wet AMD as iBRB cycling may be preserved in those with an earlier stage of the disease.

Appendix A

Munich ChronoType Questionnaire (MCTQ)

Instructions:
In this questionnaire, you report on your typical sleep behaviour over the past 4 weeks. We ask about work days and work-free days separately. Please respond to the questions according to your perception of a standard week that includes your usual work days and work-free days.

Personal Data

Date: _____

Age: _____ years

Sex: female ☐ male ☐

Height: _____ cm

Weight: _____ kg

MCTQ

I have a regular work schedule (this includes being, for example, a housewife or househusband):
Yes ☐ I work on 1☐ 2☐ 3☐ 4☐ 5☐ 6☐ 7☐ day(s) per week.
No ☐

Is your answer *"Yes, on 7 days"* or *"No"*, please consider if your sleep times may nonetheless differ between regular 'workdays' and 'weekend days' and fill out the MCTQ in this respect.

Please use 24-hour time scale (e.g. 23:00 instead of 11:00 pm)!

Workdays

Image 1: I go to bed at _____ o'clock.
Image 2: Note that some people stay awake for some time when in bed!
Image 3: I actually get ready to fall asleep at _____ o'clock.
Image 4: I need _____ minutes to fall asleep.
Image 5: I wake up at _____ o'clock.
Image 6: After _____ minutes I get up.
I use an alarm clock on workdays: Yes ☐ No ☐
If "Yes": I regularly wake up BEFORE the alarm rings: Yes ☐ No ☐

Free Days

Image 1: I go to bed at _____ o'clock.
Image 2: Note that some people stay awake for some time when in bed!
Image 3: I actually get ready to fall asleep at _____ o'clock.
Image 4: I need _____ minutes to fall asleep.
Image 5: I wake up at _____ o'clock.
Image 6: After _____ minutes I get up.
My wake-up time (Image 5) is due to the use of an alarm clock: Yes ☐ No ☐
There are particular reasons why I cannot freely choose my sleep times on free days:
Yes ☐ If "Yes": Child(ren)/pet(s) ☐ Hobbies ☐ Others ☐, for example:_____
No ☐

Work Details

In the last 3 months, I worked as a shift worker.
No ☐ Yes ☐ (please continue with "*My work schedules are ...*").

My usual work schedule …
… starts at _____ o´clock.
… ends at _____ o´clock.

My work schedules are …
… very flexible ☐ … a little flexible ☐ … rather inflexible ☐ … very inflexible ☐

I travel to work …
… within an enclosed vehicle (e.g. car, bus, underground). ☐
… not within an enclosed vehicle (e.g. on foot, by bike). ☐
I work at home. ☐

For the commute to work, I need ___ hours and ___ minutes.
For the commute from work, I need ___ hours and ___ minutes.

Stimulants

Please give approximate/average amounts!

		per →	day	/ week	/ month
I smoke	_____ cigarettes ...		☐	☐	☐
I drink	_____ glasses of beer ...		☐	☐	☐
I drink	_____ glasses of wine ...		☐	☐	☐
I drink	_____ glasses of liquor/whiskey/gin etc. ...		☐	☐	☐
I drink	_____ cups of coffee ...		☐	☐	☐
I drink	_____ cups of black tea ...		☐	☐	☐
I drink	_____ cans of caffeinated drinks (soft-drinks) ...		☐	☐	☐
I take sleep medication	_____ times ...		☐	☐	☐

Time Spent Outdoors

On average, I spend the following amount of time outdoors in daylight (without a roof above my head):
on workdays: _____ hours _____ minutes
on free days: _____ hours _____ minutes

The Munich Chronotype Questionnaire (MCTQ) used to calculate participants chronotype.

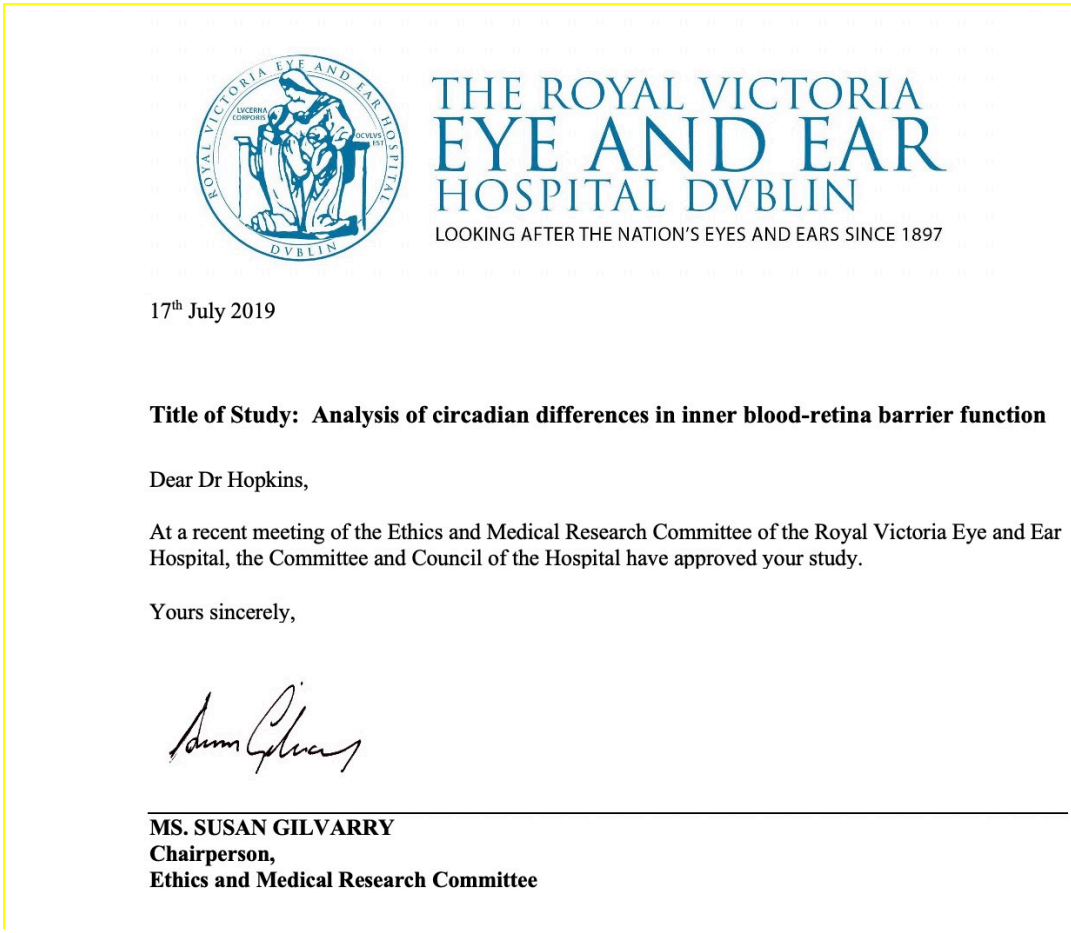

THE ROYAL VICTORIA EYE AND EAR HOSPITAL DUBLIN

LOOKING AFTER THE NATION'S EYES AND EARS SINCE 1897

17th July 2019

Title of Study: Analysis of circadian differences in inner blood-retina barrier function

Dear Dr Hopkins,

At a recent meeting of the Ethics and Medical Research Committee of the Royal Victoria Eye and Ear Hospital, the Committee and Council of the Hospital have approved your study.

Yours sincerely,

MS. SUSAN GILVARRY
Chairperson,
Ethics and Medical Research Committee

Letter from the Research and Ethics (REC) Committee in The Royal Victoria Eye and ear Hospital confirming ethical approval for the project. The letter is addressed to Dr Alan Hopkins, a research fellow who is also involved in the project.

CONVERSION TABLE FOR LOGMAR TO SNELLEN'S EQUIVALENT

LOGMAR	SNELLEN EQUIVALENT
1.0	6/60
0.9	6/48
0.8	6/38
0.7	6/30
0.6	6/24
0.5	6/19
0.4	6/15
0.3	6/12
0.2	6/9.5
0.1	6/7.5
0.0	6/6
-0.1	6/5
-0.2	6/4
-0.3	6/3

Nb Each line on the chart represents a change of 0.1 log unit in the acuity level with each letter having a value of 0.02 log unit.
Therefore a patient reading correctly all letters on a specific line will score the full 0.1 log unit. For every extra letter on subsequent lines the patient reads correctly the patient will score an extra -0.02

The table used to convert participants' visual acuity from Snellen to LogMAR.

References

A randomized, placebo-controlled, clinical trial of high-dose supplementation with vitamins C and E, beta carotene, and zinc for age-related macular degeneration and vision loss: AREDS report no. 8. (2001). Arch Ophthalmol, 119(10), 1417-1436. doi:10.1001/archopht.119.10.1417

Agnifili, L., Mastropasqua, R., Frezzotti, P., Fasanella, V., Motolese, I., Pedrotti, E., Iorio, A.D., Mattei, P.A., Motolese, E. & Mastropasqua, L. (2015), Circadian intraocular pressure patterns in healthy subjects, primary open angle and normal tension glaucoma patients with a contact lens sensor. Acta Ophthalmol, 93: e14-e21. https://doi.org/10.1111/aos.12408

Arya, M., Sabrosa, A. S., Duker, J. S., & Waheed, N. K. (2018). Choriocapillaris changes in dry age-related macular degeneration and geographic atrophy: a review. Eye and vision (London, England), 5, 22-22. doi:10.1186/s40662-018-0118-x

Barondes, M., Pauleikhoff, D., Chisholm, I. C., Minassian, D., & Bird, A. C. (1990). Bilaterality of drusen. Br J Ophthalmol, 74(3), 180-182. doi:10.1136/bjo.74.3.180

Bazzoni, G., & Dejana, E. (2004). Endothelial cell-to-cell junctions: molecular organization and role in vascular homeostasis. Physiol Rev, 84(3), 869-901. doi:10.1152/physrev.00035.2003

Bazzoni, G., Martinez-Estrada, O. M., Orsenigo, F., Cordenonsi, M., Citi, S., & Dejana, E. (2000). Interaction of junctional adhesion molecule with the tight junction components ZO-1, cingulin, and occludin. J Biol Chem, 275(27), 20520-20526. doi:10.1074/jbc.M905251199

Bird, A. C. (1992). Bruch's membrane change with age. The British journal of ophthalmology, 76(3), 166-168. doi:10.1136/bjo.76.3.166

Bird, A. C., Bressler, N. M., Bressler, S. B., Chisholm, I. H., Coscas, G., Davis, M. D., . . . et al. (1995). An international classification and grading system for age-related maculopathy and age-related macular degeneration. The International ARM Epidemiological Study Group. Surv Ophthalmol, 39(5), 367-374. doi:10.1016/s0039-6257(05)80092-x

Bokinni, Y., Shah, N., Maguire, O., & Laidlaw, D. A. (2015). Performance of a computerised visual acuity measurement device in subjects with age-related macular degeneration: comparison with gold standard ETDRS chart measurements. Eye (Lond), 29(8), 1085-1091. doi:10.1038/eye.2015.94

Bonini Filho, M. A. W., A.J. (2015). Outer retinal layers as predictors of vision loss. Rev Ophthalmol.

Boyle, D., Tien, L. F., Cooper, N. G., Shepherd, V., & McLaughlin, B. J. (1991). A mannose receptor is involved in retinal phagocytosis. Invest Ophthalmol Vis Sci, 32(5), 1464-1470.

Cahill, M. T., Mruthyunjaya, P., Bowes Rickman, C., & Toth, C. A. (2005). Recurrence of retinal pigment epithelial changes after macular translocation with 360 degrees peripheral retinectomy for geographic atrophy. Arch Ophthalmol, 123(7), 935-938. doi:10.1001/archopht.123.7.935

Campbell, M., & Humphries, P. (2012). The blood-retina barrier: tight junctions and barrier modulation. Adv Exp Med Biol, 763, 70-84.

Casten, R. J., & Rovner, B. W. (2013). Update on depression and age-related macular degeneration. Current opinion in ophthalmology, 24(3), 239-243. doi:10.1097/ICU.0b013e32835f8e55

Chakravarthy, U., Wong, T. Y., Fletcher, A., Piault, E., Evans, C., Zlateva, G., . . . Mitchell, P. (2010). Clinical risk factors for age-related macular degeneration: a systematic review and meta-analysis. BMC ophthalmology, 10, 31-31. doi:10.1186/1471-2415-10-31

Chew, E. Y., Lindblad, A. S., & Clemons, T. (2009). Summary results and recommendations from the age-related eye disease study. Arch Ophthalmol, 127(12), 1678-1679. doi:10.1001/archophthalmol.2009.312

Colegio, O. R., Van Itallie, C., Rahner, C., & Anderson, J. M. (2003). Claudin extracellular domains determine paracellular charge selectivity and resistance but not tight junction fibril architecture. Am J Physiol Cell Physiol, 284(6), C1346-1354. doi:10.1152/ajpcell.00547.2002

Connolly, E., Rhatigan, M., O'Halloran, A. M., Muldrew, K. A., Chakravarthy, U., Cahill, M., . . . Doyle, S. L. (2018). Prevalence of age-related macular degeneration associated genetic risk factors and 4-year progression data in the Irish population. Br J Ophthalmol, 102(12), 1691-1695. doi:10.1136/bjophthalmol-2017-311673

Cook, H. L., Patel, P. J., & Tufail, A. (2008). Age-related macular degeneration: diagnosis and management. Br Med Bull, 85, 127-149. doi:10.1093/bmb/ldn012

Crabb, J. W., Miyagi, M., Gu, X., Shadrach, K., West, K. A., Sakaguchi, H., . . . Hollyfield, J. G. (2002). Drusen proteome analysis: an approach to the etiology of age-related macular degeneration. Proceedings of the National Academy of Sciences of the United States of America, 99(23), 14682-14687. doi:10.1073/pnas.222551899

Cunha-Vaz, J., Bernardes, R., & Lobo, C. (2011). Blood-retinal barrier. Eur J Ophthalmol, 21 Suppl 6, S3-9. doi:10.5301/ejo.2010.6049

Curcio, C. A. (2018). Antecedents of Soft Drusen, the Specific Deposits of Age-Related Macular Degeneration, in the Biology of Human Macula. Invest Ophthalmol Vis Sci, 59(4), Amd182-amd194. doi:10.1167/iovs.18-24883

Curcio, C. A., Johnson, M., Huang, J. D., & Rudolf, M. (2009). Aging, age-related macular degeneration, and the response-to-retention of apolipoprotein B-containing lipoproteins. Progress in retinal and eye research, 28(6), 393-422. doi:10.1016/j.preteyeres.2009.08.001

Curcio, C. A., Medeiros, N. E., & Millican, C. L. (1996). Photoreceptor loss in age-related macular degeneration. Invest Ophthalmol Vis Sci, 37(7), 1236-1249.

Curcio, C. A., Owsley, C., & Jackson, G. R. (2000). Spare the rods, save the cones in aging and age-related maculopathy. Invest Ophthalmol Vis Sci, 41(8), 2015-2018.

Daneman, R., Zhou, L., Agalliu, D., Cahoy, J. D., Kaushal, A., & Barres, B. A. (2010). The mouse blood-brain barrier transcriptome: a new resource for understanding the development and function of brain endothelial cells. PLoS One, 5(10), e13741. doi:10.1371/journal.pone.0013741

Daruich, A., Matet, A., Moulin, A., Kowalczuk, L., Nicolas, M., Sellam, A., . . . Behar-Cohen, F. (2018). Mechanisms of macular edema: Beyond the surface. Progress in retinal and eye research, 63, 20-68. doi:10.1016/j.preteyeres.2017.10.006

Dierickx, P., Van Laake, L. W., & Geijsen, N. (2018). Circadian clocks: from stem cells to tissue homeostasis and regeneration. EMBO Rep, 19(1), 18-28. doi:10.15252/embr.201745130

Drance, S. M. (1963) Diurnal Variation of Intraocular Pressure in Treated Glaucoma: Significance in Patients With Chronic Simple Glaucom. Arch Ophthalmol, 70(3), 302–311. doi:10.1001/archopht.1963.00960050304004

Ehrlich, R., Harris, A., Kheradiya, N. S., Winston, D. M., Ciulla, T. A., & Wirostko, B. (2008). Age-related macular degeneration and the aging eye. Clinical interventions in aging, 3(3), 473-482. doi:10.2147/cia.s2777

Falkenstein, I. A., Cochran, D. E., Azen, S. P., Dustin, L., Tammewar, A. M., Kozak, I., & Freeman, W. R. (2008). Comparison of visual acuity in macular degeneration patients measured with snellen and early treatment diabetic retinopathy study charts. Ophthalmology, 115(2), 319-323. doi:10.1016/j.ophtha.2007.05.028

Fanjul-Moles, M. L., & Lopez-Riquelme, G. O. (2016). Relationship between Oxidative Stress, Circadian Rhythms, and AMD. Oxid Med Cell Longev, 2016, 7420637. doi:10.1155/2016/7420637

Ferris, F. L., Davis, M. D., Clemons, T. E., Lee, L.-Y., Chew, E. Y., Lindblad, A. S., . . . Age-Related Eye Disease Study Research, G. (2005). A simplified severity scale for age-related macular degeneration: AREDS Report No. 18. Archives of ophthalmology (Chicago, Ill. : 1960), 123(11), 1570-1574. doi:10.1001/archopht.123.11.1570

Fleckenstein, M., Mitchell, P., Freund, K. B., Sadda, S., Holz, F. G., Brittain, C., . . . Ferrara, D. (2018). The Progression of Geographic Atrophy Secondary to Age-Related Macular Degeneration. Ophthalmology, 125(3), 369-390. doi:10.1016/j.ophtha.2017.08.038

Forrester, J. V., Dick, A. D., McMenamin, P. G., Roberts, F., & Eric Pearlman, B. S. (2015). The Eye: Basic Sciences in Practice: Elsevier Health Sciences.

Fragiotta, S., Fernández-Avellaneda, P., Breazzano, M. P., Curcio, C. A., Leong, B. C. S., Kato, K., . . . Freund, K. B. (2019). The Fate and Prognostic Implications of Hyperreflective Crystalline Deposits in Nonneovascular Age-Related Macular Degeneration. Investigative Ophthalmology & Visual Science, 60(8), 3100-3109. doi:10.1167/iovs.19-26589

Frank, R. N., Schulz, L., Abe, K., & Iezzi, R. (2004). Temporal variation in diabetic macular edema measure by optical coherence tomography. Ophthalmology, 111(2), 211-217. doi: 10.1016/j.ophtha.2003.05.031

Fritsche, L. G., Fariss, R. N., Stambolian, D., Abecasis, G. R., Curcio, C. A., & Swaroop, A. (2014). Age-related macular degeneration: genetics and biology coming together. Annual review of genomics and human genetics, 15, 151-171. doi:10.1146/annurev-genom-090413-025610

García-Layana, A., Cabrera-López, F., García-Arumí, J., Arias-Barquet, L., & Ruiz-Moreno, J. M. (2017). Early and intermediate age-related macular degeneration: update and clinical review. Clinical interventions in aging, 12, 1579-1587. doi:10.2147/cia.S142685

González-Mariscal, L., Betanzos, A., & Avila-Flores, A. (2000). MAGUK proteins: structure and role in the tight junction. Semin Cell Dev Biol, 11(4), 315-324. doi:10.1006/scdb.2000.0178

Gopinath, B., Liew, G., Burlutsky, G., & Mitchell, P. (2014). Age-related macular degeneration and 5-year incidence of impaired activities of daily living. Maturitas, 77(3), 263-266. doi:https://doi.org/10.1016/j.maturitas.2013.12.001

Green, D., Ducorroy, G., McElnea, E., Naughton, A., Skelly, A., O'Neill, C., . . . Keegan, D. (2016). The Cost of Blindness in the Republic of Ireland 2010–2020. Journal of Ophthalmology, 2016, 4691276. doi:10.1155/2016/4691276

Gupta, B., Grewal, J., Adewoyin, T., Pelosini, L. & Williamson, T.H. (2008). Diurnal variation of macular oedema in CRVO: prospective study. Graefes Arch Clin Exp Ophthalmol, 247, 593. doi: 10.1007/s00417-008-1011-4

Han, Y. S., Lim, H. B., Lee, S. H. & Kim, J. Y. (2015). Thickness of the Early Treatment of Diabetic Retinopathy Study macular subfields determined using swept-source optical coherence tomography. Ophthalmologica, 233, 192-197. doi: 10.1159/000375538

Heesterbeek, T. J., Lores-Motta, L., Hoyng, C. B., Lechanteur, Y. T. E., & den Hollander, A. I. (2020). Risk factors for progression of age-related macular degeneration. Ophthalmic Physiol Opt, 40(2), 140-170. doi:10.1111/opo.12675

Hood, S., & Amir, S. (2017). The aging clock: circadian rhythms and later life. J Clin Invest, 127(2), 437-446. doi:10.1172/jci90328

Hudson, N., Celkova, L., Hopkins, A., Greene, C., Storti, F., Ozaki, E., . . . Campbell, M. (2019). Dysregulated claudin-5 cycling in the inner retina causes retinal pigment epithelial cell atrophy. JCI Insight, 4(15). doi:10.1172/jci.insight.130273

Hussain, B., Saleh, G. M., Sivaprasad, S., & Hammond, C. J. (2006). Changing from Snellen to LogMAR: debate or delay? Clin Exp Ophthalmol, 34(1), 6-8. doi:10.1111/j.1442-9071.2006.01135

Hossein, A. & Nowroozzadeh, M. H. (2014). Diurnal variation of retinal thickness in healthy subjects. Optom Vis Sci, 91(6), 615-623. doi: 10.1097/OPX.0000000000000269

INVOLVE. (2012). Briefing notes for researchers: involving the public in NHS, public health and social care research. Retrieved from Eastleigh:

Kastin, A. J., & Pan, W. (2016). Involvement of the Blood-Brain Barrier in Metabolic Regulation. CNS Neurol Disord Drug Targets, 15(9), 1118-1128. doi:10.2174/1871527315666160920124928

Khan, K. N., Mahroo, O. A., Khan, R. S., Mohamed, M. D., McKibbin, M., Bird, A., . . . Moore, A. T. (2016). Differentiating drusen: Drusen and drusen-like appearances associated with ageing, age-related macular degeneration, inherited eye disease and other pathological processes. Progress in retinal and eye research, 53, 70-106. doi:https://doi.org/10.1016/j.preteyeres.2016.04.008

Kim, J. Y., Zhao, H., Martinez, J., Doggett, T. A., Kolesnikov, A. V., Tang, P. H., . . . Ferguson, T. A. (2013). Noncanonical autophagy promotes the visual cycle. Cell, 154(2), 365-376. doi:10.1016/j.cell.2013.06.012

Klein, R., Klein, B. E., Tomany, S. C., Meuer, S. M., & Huang, G. H. (2002). Ten-year incidence and progression of age-related maculopathy: The Beaver Dam eye study. Ophthalmology, 109(10), 1767-1779. doi:10.1016/s0161-6420(02)01146-6

Kofuji, P., Mure, L. S., Massman, L. J., Purrier, N., Panda, S., & Engeland, W. C. (2016). Intrinsically Photosensitive Retinal Ganglion Cells (ipRGCs) Are Necessary for Light Entrainment of Peripheral Clocks. PLoS One, 11(12), e0168651. doi:10.1371/journal.pone.0168651

Laurent, V., Sengupta, A., Sánchez-Bretaño, A., Hicks, D., & Tosini, G. (2017). Melatonin signaling affects the timing in the daily rhythm of phagocytic activity by the retinal pigment epithelium. Experimental eye research, 165, 90-95. doi:10.1016/j.exer.2017.09.007

LaVail, M. (1976). Rod outer segment disk shedding in rat retina: relationship to cyclic lighting. Science, 194(4269), 1071-1074. doi:10.1126/science.982063

Levandovski, R., Sasso, E., & Hidalgo, M. P. (2013). Chronotype: a review of the advances, limits and applicability of the main instruments used in the literature to assess human phenotype. Trends in Psychiatry and Psychotherapy, 35, 3-11. Retrieved from http://www.scielo.br/scielo.php?script=sci_arttext&pid=S2237-60892013000100002&nrm=iso

Liu, J.H., Zhang, X., Kripke, D.F., Weinreb, R.N. (2003). Twenty-four-hour intraocular pressure pattern associated with early glaucomatous changes. Invest Ophthalmol Vis Sci, 44(4),1586-90. doi: 10.1167/iovs.02-0666.

Ly, A., Nivison-Smith, L., Assaad, N., & Kalloniatis, M. (2017). Fundus Autofluorescence in Age-related Macular Degeneration. Optom Vis Sci, 94(2), 246-259. doi:10.1097/opx.0000000000000997

Mann, S. S., Rutishauser-Arnold, Y., Peto, T., Jenkins, S. A., Leung, I., Xing, W., . . . Webster, A. R. (2011). The symmetry of phenotype between eyes of patients with early and late bilateral age-related macular degeneration (AMD). Graefes Arch Clin Exp Ophthalmol, 249(2), 209-214. doi:10.1007/s00417-010-1483-x

Mansouri, K., Tanna, A. P., De Morales, C. G., Camp, A. S., & Weinreb, R. N. (2020). Review of the measurement of 24-hour intraocular pressure in patients with glaucoma. Serv Ophthalmol, 65(2), 171-186. doi: /10.1016/j.survophthal.2019.09.004

Marneros, A. G., Fan, J., Yokoyama, Y., Gerber, H. P., Ferrara, N., Crouch, R. K., & Olsen, B. R. (2005). Vascular Endothelial Growth Factor Expression in the Retinal Pigment Epithelium Is Essential for Choriocapillaris Development and Visual Function. The American journal of pathology, 167(5), 1451-1459. doi:10.1016/S0002-9440(10)61231-X

McLeod, D. S., Grebe, R., Bhutto, I., Merges, C., Baba, T., & Lutty, G. A. (2009). Relationship between RPE and choriocapillaris in age-related macular degeneration. Investigative Ophthalmology & Visual Science, 50(10), 4982-4991. doi:10.1167/iovs.09-3639

Mitchell, P., Liew, G., Gopinath, B., & Wong, T. Y. (2018). Age-related macular degeneration. The Lancet, 392(10153), 1147-1159. doi:10.1016/S0140-6736(18)31550-2

Mitchell, P., Wang, J. J., Smith, W., & Leeder, S. R. (2002). Smoking and the 5-Year Incidence of Age-Related Maculopathy: The Blue Mountains Eye Study. Archives of Ophthalmology, 120(10), 1357-1363. doi:10.1001/archopht.120.10.1357

Morita, K., Sasaki, H., Furuse, M., & Tsukita, S. (1999). Endothelial Claudin: Claudin-5/Tmvcf Constitutes Tight Junction Strands in Endothelial Cells. Journal of Cell Biology, 147(1), 185-194. doi:10.1083/jcb.147.1.185

Nandrot, E. F., Kim, Y., Brodie, S. E., Huang, X., Sheppard, D., & Finnemann, S. C. (2004). Loss of synchronized retinal phagocytosis and age-related blindness in mice lacking alphavbeta5 integrin. The Journal of experimental medicine, 200(12), 1539-1545. doi:10.1084/jem.20041447

Naylor, A., Hopkins, A., Hudson, N., & Campbell, M. (2019). Tight Junctions of the Outer Blood Retina Barrier. International journal of molecular sciences, 21(1). doi:10.3390/ijms21010211

Nitta, T., Hata, M., Gotoh, S., Seo, Y., Sasaki, H., Hashimoto, N., . . . Tsukita, S. (2003). Size-selective loosening of the blood-brain barrier in claudin-5-deficient mice. The Journal of cell biology, 161(3), 653-660. doi:10.1083/jcb.200302070

Peng, S., Adelman, R. A., & Rizzolo, L. J. (2010). Minimal effects of VEGF and anti-VEGF drugs on the permeability or selectivity of RPE tight junctions. Invest Ophthalmol Vis Sci, 51(6), 3216-3225. doi:10.1167/iovs.09-4162

Pennington, K. L., & DeAngelis, M. M. (2016). Epidemiology of age-related macular degeneration (AMD): associations with cardiovascular disease phenotypes and lipid factors. Eye and vision (London, England), 3, 34-34. doi:10.1186/s40662-016-0063-5

Power, W. B., P.; Moriarty, P.; Kelly, S. (2017). Model of Eye Care. Retrieved from

Read, S. A., Collins, M. J., & Alonso-Caneiro, D. (2012). Diurnal variation of retinal thickness with spectral domain OCT. Optom Vis Sci, 89(5), 611-619. doi:10.1097/OPX.0b013e3182501917

Rizzolo, L. J., Peng, S., Luo, Y., & Xiao, W. (2011). Integration of tight junctions and claudins with the barrier functions of the retinal pigment epithelium. Progress in retinal and eye research, 30(5), 296-323. doi:10.1016/j.preteyeres.2011.06.002

Roenneberg, T., Kuehnle, T., Juda, M., Kantermann, T., Allebrandt, K., Gordijn, M., & Merrow, M. (2007). Epidemiology of the human circadian clock. Sleep Med Rev, 11(6), 429-438. doi:10.1016/j.smrv.2007.07.005

Roenneberg, T., Pilz, L. K., Zerbini, G., & Winnebeck, E. C. (2019). Chronotype and Social Jetlag: A (Self-) Critical Review. Biology (Basel), 8(3). doi:10.3390/biology8030054

Rosen, R., Hu, D.-N., Perez, V., Tai, K., Yu, G.-P., Chen, M., . . . Walsh, J. (2009). Urinary 6-sulfatoxymelatonin level in age-related macular degeneration patients. Molecular vision, 15, 1673-1679. Retrieved from https://pubmed.ncbi.nlm.nih.gov/19710945

https://www.ncbi.nlm.nih.gov/pmc/articles/PMC2730752/

Rosenfeld, P. J., Brown, D. M., Heier, J. S., Boyer, D. S., Kaiser, P. K., Chung, C. Y., & Kim, R. Y. (2006). Ranibizumab for Neovascular Age-Related Macular Degeneration. New England Journal of Medicine, 355(14), 1419-1431. doi:10.1056/NEJMoa054481

Rudolf, M., Clark, M. E., Chimento, M. F., Li, C.-M., Medeiros, N. E., & Curcio, C. A. (2008). Prevalence and Morphology of Druse Types in the Macula and Periphery of Eyes with Age-Related Maculopathy. Investigative Ophthalmology & Visual Science, 49(3), 1200-1209. doi:10.1167/iovs.07-1466

Ryu, H., Joo, E. Y., Choi, S. J., & Suh, S. (2018). Validation of the Munich ChronoType Questionnaire in Korean Older Adults. Psychiatry Investig, 15(8), 775-782. doi:10.30773/pi.2018.04.09

Saitou, M., Furuse, M., Sasaki, H., Schulzke, J. D., Fromm, M., Takano, H., . . . Tsukita, S. (2000). Complex phenotype of mice lacking occludin, a component of tight junction strands. Mol Biol Cell, 11(12), 4131-4142. doi:10.1091/mbc.11.12.4131

Shin, K., Fogg, V. C., & Margolis, B. (2006). Tight junctions and cell polarity. Annu Rev Cell Dev Biol, 22, 207-235. doi:10.1146/annurev.cellbio.22.010305.104219

Simó, R., Villarroel, M., Corraliza, L., Hernández, C., & Garcia-Ramírez, M. (2010). The Retinal Pigment Epithelium: Something More than a Constituent of the Blood-Retinal Barrier—Implications for the Pathogenesis of Diabetic Retinopathy. Journal of Biomedicine and Biotechnology, 2010, 190724. doi:10.1155/2010/190724

Sparrrow, J. R., Hicks, D., & Hamel, C. P. (2010). The Retinal Pigment Epithelium in Health and Disease. Current Molecular Medicine, 10(9), 802-823. doi:http://dx.doi.org/10.2174/156652410793937813

Stefánsson, E., Geirsdóttir, Á., & Sigurdsson, H. (2011). Metabolic physiology in age related macular degeneration. Progress in retinal and eye research, 30(1), 72-80. doi:https://doi.org/10.1016/j.preteyeres.2010.09.003

Stepicheva, N. A., Weiss, J., Shang, P., Yazdankhah, M., Ghosh, S., Bhutto, I. A., . . . Sinha, D. (2019). Melatonin as the Possible Link Between Age-Related Retinal Regeneration and the Disrupted Circadian Rhythm in Elderly. Adv Exp Med Biol, 1185, 45-49. doi:10.1007/978-3-030-27378-1_8

Sternberg Jr, P. d. B., S.; Lim, J.I.; Rezaei, K.; Saperstein, D.A. (Producer). (2017, 16/06/2020). Age Related Macular Degeneration: Introduction.

Strauss, O. (2005). The retinal pigment epithelium in visual function. Physiol Rev, 85(3), 845-881. doi:10.1152/physrev.00021.2004

Sundaram, V., ; Barsam, A.; Barker, L.; Khaw, P.T. (2016). Training in ophthalmology the essential clinical cirriculum (Second Edition ed.). New York: Oxford University Press.

Terman, J. S., Terman, M., Lo, E. S., & Cooper, T. B. (2001). Circadian time of morning light administration and therapeutic response in winter depression. Arch Gen Psychiatry, 58(1), 69-75. doi:10.1001/archpsyc.58.1.69

Tosini, G., & Menaker, M. (1996). Circadian rhythms in cultured mammalian retina. Science, 272(5260), 419-421. doi:10.1126/science.272.5260.419

Usui, S., Ikuno, Y., Akiba, M., Maruko, I., Sekiryu, T., Nishida, K., & Iida, T. (2012). Circadian changes in subfoveal choroidal thickness and the relationship with circulatory factors in healthy subjects. Invest Ophthalmol Vis Sci, 53(4), 2300-2307. doi:10.1167/iovs.11-8383

Vallée, A., Lecarpentier, Y., Vallée, R., Guillevin, R., & Vallée, J.-N. (2020). Circadian Rhythms in Exudative Age-Related Macular Degeneration: The Key Role of the Canonical WNT/β-Catenin Pathway. International journal of molecular sciences, 21(3), 820. doi:10.3390/ijms21030820

Velilla, S., García-Medina, J. J., García-Layana, A., Dolz-Marco, R., Pons-Vázquez, S., Pinazo-Durán, M. D., . . . Gallego-Pinazo, R. (2013). Smoking and age-related macular degeneration: review and update. Journal of Ophthalmology, 2013, 895147-895147. doi:10.1155/2013/895147

Wang, L., Clark, M. E., Crossman, D. K., Kojima, K., Messinger, J. D., Mobley, J. A., & Curcio, C. A. (2010). Abundant lipid and protein components of drusen. PLoS One, 5(4), e10329. doi:10.1371/journal.pone.0010329

Wightman, A. J., & Guymer, R. H. (2019). Reticular pseudodrusen: current understanding. Clinical and Experimental Optometry, 102(5), 455-462. doi:10.1111/cxo.12842

Wong, W. L., Su, X., Li, X., Cheung, C. M. G., Klein, R., Cheng, C.-Y., & Wong, T. Y. (2014). Global prevalence of age-related macular degeneration and disease burden projection for 2020 and 2040: a systematic review and meta-analysis. The Lancet Global Health, 2(2), e106-e116. doi:10.1016/S2214-109X(13)70145-1

Yao, J., Qiu, Y., Frontera, E., Jia, L., Khan, N. W., Klionsky, D. J., . . . Zacks, D. N. (2018). Inhibiting autophagy reduces retinal degeneration caused by protein misfolding. Autophagy, 14(7), 1226-1238. doi:10.1080/15548627.2018.1463121

Yi, C., Pan, X., Yan, H., Guo, M., & Pierpaoli, W. (2005). Effects of melatonin in age-related macular degeneration. Ann N Y Acad Sci, 1057, 384-392. doi:10.1196/annals.1356.029

Young-Joon, J., Dong-Won, H., Yong-IL, S., Jung-Yeul, K. (2016) Diurnal Variation of Retina Thickness Measured with Time Domain and Spectral Domain Optical Coherence Tomography in Healthy Subjects. Invest Ophthalmol Vis Sci, 52(9), 6497-6500. doi: https://doi.org/10.1167/iovs.11-7403.

Zhou, Q., Daniel, E., Maguire, M. G., Grunwald, J. E., Martin, E. R., Martin, D. F., & Ying, G.-s. (2016). Pseudodrusen and Incidence of Late Age-Related Macular Degeneration in Fellow Eyes in the Comparison of Age-Related Macular Degeneration Treatments Trials. Ophthalmology, 123(7), 1530-1540. doi:https://doi.org/10.1016/j.ophtha.2016.02.043

Zweifel, S. A., Spaide, R. F., Curcio, C. A., Malek, G., & Imamura, Y. (2010). Reticular Pseudodrusen Are Subretinal Drusenoid Deposits. *Ophthalmology, 117*(2), 303-312.e301. doi:10.1016/j.ophtha.2009.07.014